

110 T

Cours/Lecture Series

1982-1983 ACADEMIC TRAINING PROGRAMME

Title "Permanent magnet technology"

Lecturer W. BARAN (Krupp Institute, Essen)

Dates October 21 & 22, 1982

Time 10h30 to 12h30

Place Auditorium

Abstract Theory of permanent magnet state.

Permanent magnet materials, manufacturing processes and properties : hard ferrites, AlNiCo, rare earth metal-cobalt (RECo), other.

Design of permanent magnet circuits : conventional, analytical and numerical methods.

Typical permanent magnet circuits and applications, with emphasis on RECo-devices in particle optics.

Distr.: int. + ext.

CERN LIBRARIES, GENEVA



CM-P00073149

Training & Education Service
Secretariat: Tel. 2844
PE/ED/TE

COPIES OF
TRANSPARENCIES

The permanent magnet circuit

1. Materials

1.1. Permanent magnet materials

1.1.1. Theory of permanent magnet state

1.1.2. Manufacturing and properties

AlNiCo

Hard ferrite

RE-Co

Other

1.1.3. Magnetizing

1.1.4. Influences on permanent magnets

Magnetic fields

Temperature

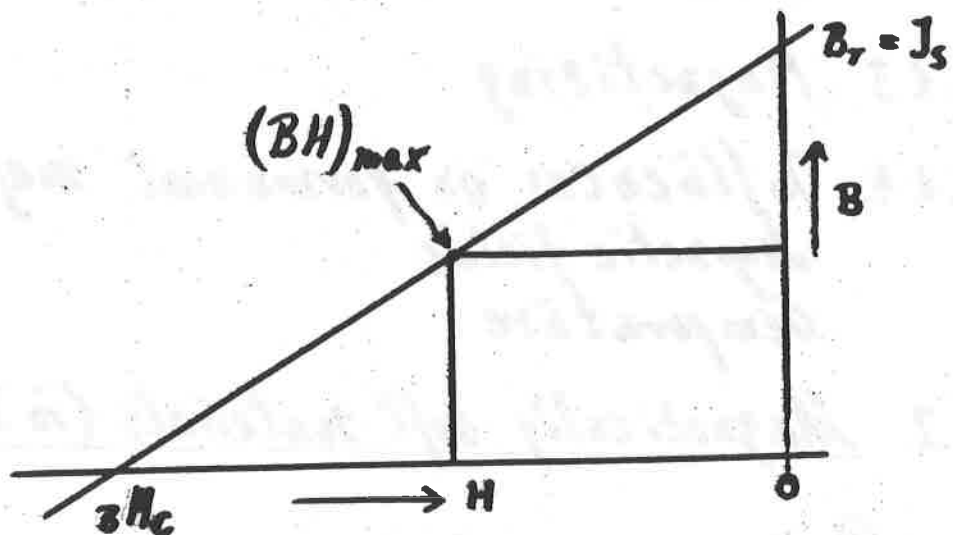
1.2. Magnetically soft materials (in PM circuit)

2. Design

3. Applications

The ideal permanent magnet.

1. high $B_r \rightarrow \underline{\text{high } J_s}$ / *Primary properties*
2. high $J_s H_c \rightarrow \begin{cases} \text{high anisotropy} \\ \text{no moving Bloch-walls} \end{cases}$
3. $\mu_{\text{rev}} = 1 \}$ $B_r = J_s \} \rightarrow \begin{matrix} \text{same anisotropy} \\ \text{direction for the} \\ \text{whole magnet} \end{matrix}$



Theoretical maximum: $J_s^2 / 4\mu_0$

$$J_s = 2,4 T \longrightarrow (BH)_{\text{max}} = 1200 \frac{kT}{m^3}$$

| crystal anisotropy
shape " "

Material	Herstellverfahren für anisotrope Dauermagnete	Energieinhalt kJ/m ³
AlNiCo (KOERZIT)	<p>Pulver → Pressen → Sintern → Wärmebehandlung im Magnetf.</p>	40
Hartferrit (KOEROX) SECo ₅ (KOERMAX) SE ₂ (Co, Mn) ₁₇	<p>Pulver → Pressen im Magnetfeld → Sintern</p>	30 160 220
MnAlC	<p>Gussblock → Warmfließpressen</p>	50

1. Crystal anisotropy.

In each crystallite magnetization fixed to some directions.

2. Shape anisotropy

Two (or more) phases with different saturation magnetization.

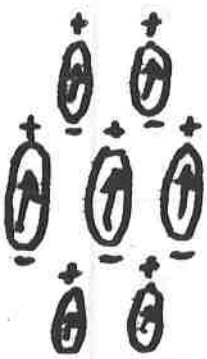
Magnetoelastic energy (ME) is minimized, for magnetization in the long direction.

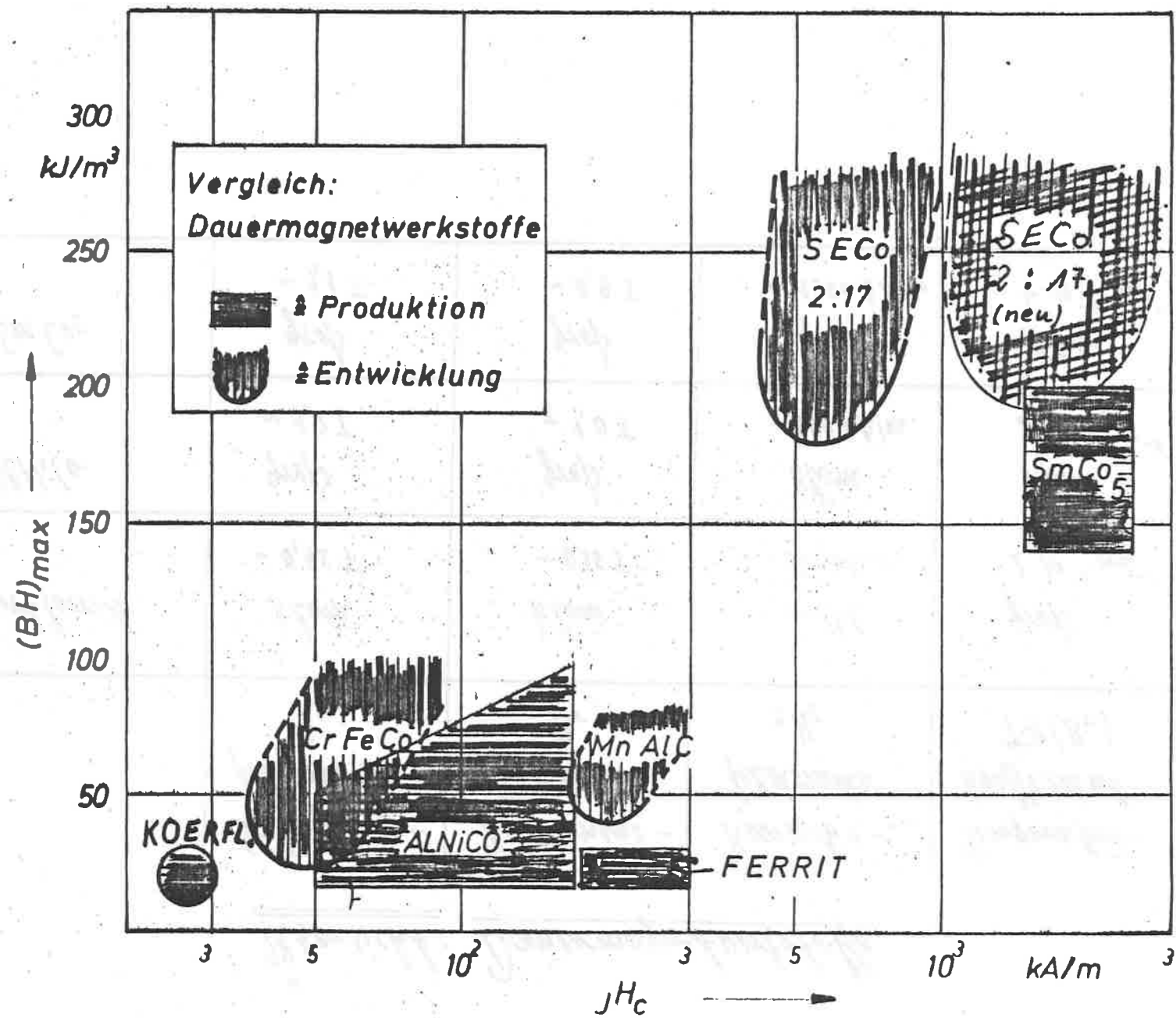
By packing reduction of ME.

Maximum for 75% packing fraction.

$\Rightarrow \frac{5}{16}$ of maximum energy product.

3. Strain anisotropy (important)





Übersicht: Dauermagnetwerkstoffe

	Sättigungspolarisation J_s	Remanenzflussdichte B_r	Koerzitivfeldstärke μH_c	Temperaturkoeffizient $TK(B_r)$
Hartferrit	klein ~ 0,45 T	klein ~ 0,35 T	mittel ~ 300 kA/m	gross $2 \cdot 10^{-3} \text{ grad}^{-1}$
AlNiCo	gross ~ 1,2 T	gross ~ 1,0 T	klein ~ 100 kA/m	klein $2 \cdot 10^{-4} \text{ grad}^{-1}$
SmCo ₅	gross ~ 1,1 T	gross ~ 0,9 T	gross ~ 1500 kA/m	klein $4 \cdot 10^{-4} \text{ grad}^{-1}$

Dauermagnetwerkstoff aus Seltenerdmetall und Kobalt

Vorbemerkung

KOERMAX ist ein pulvermetallurgisch hergestellter, anisotroper Dauermagnetwerkstoff aus Seltenerdmetallen und Kobalt mit ausgezeichneten magnetischen Eigenschaften. Er übertrifft bei hoher Sättigungspolarisation alle bisher eingesetzten Dauermagnetwerkstoffe im maximalen Energieprodukt und in der Koerzitivfeldstärke und bildet daher die sinnvolle Ergänzung der bekannten KRUPP Dauermagnetwerkstoffe **KOERZIT**, **KOEROX** und **KOERFLEX**. KRUPP WIDIA liefert die Sorten **KOERMAX 130** und **KOERMAX 160** mit typischen Werten des maximalen Energieproduktes von 130 und 160 kJ/m³. Über den Einsatz der Sorten entscheiden die magnetischen Anforderungen sowie Größe und Form der Magnete.

Magnetische Kennwerte

In der Tabelle 1 sind die magnetischen Werte der beiden Sorten in ihren typischen Streubreiten wiedergegeben. **KOERMAX 130** entspricht der einzigen in der DIN 17410 aufgeführten Seltenerdmetall-Kobalt-Sorte SECo 112/100, bei **KOERMAX 160** wurde zur weiteren Kennzeichnung der Kurzname in Anlehnung an DIN 17410 gewählt. In Bild 1 werden typische Entmagnetisierungskurven von **KOERMAX 130** und **KOERMAX 160**, der AlNiCo-Legierung **KOERZIT 500** und des Hartferritwerkstoffes **KOEROX 330** dargestellt. Die überragenden magnetischen Eigenschaften von **KOERMAX** sind deutlich zu erkennen.

Tabelle 1: Magnetische Kennwerte von **KOERMAX**

Sorte	Kennzeichnung nach DIN 17410	Maximales Energieprodukt $(BH)_{max}$ kJ/m ³	Remanenzflußdichte B_r mT	Koerzitivfeldstärke H_c kA/m	J_{Hc} kA/m	Relative permanente Permeabilität μ_p
KOERMAX 130	SECo 112/100	110–140	750–840	520–620	> 1000	≤ 1,1
KOERMAX 160	SECo 140/120	140–180	840–950	580–730	> 1200	≤ 1,1

Zur Umrechnung in die bisher gebräuchlichen Einheiten:
1 kJ/m³ = 0,126 MGoe, 1 mT = 10 G, 1 kA/m = 12,6 Oe

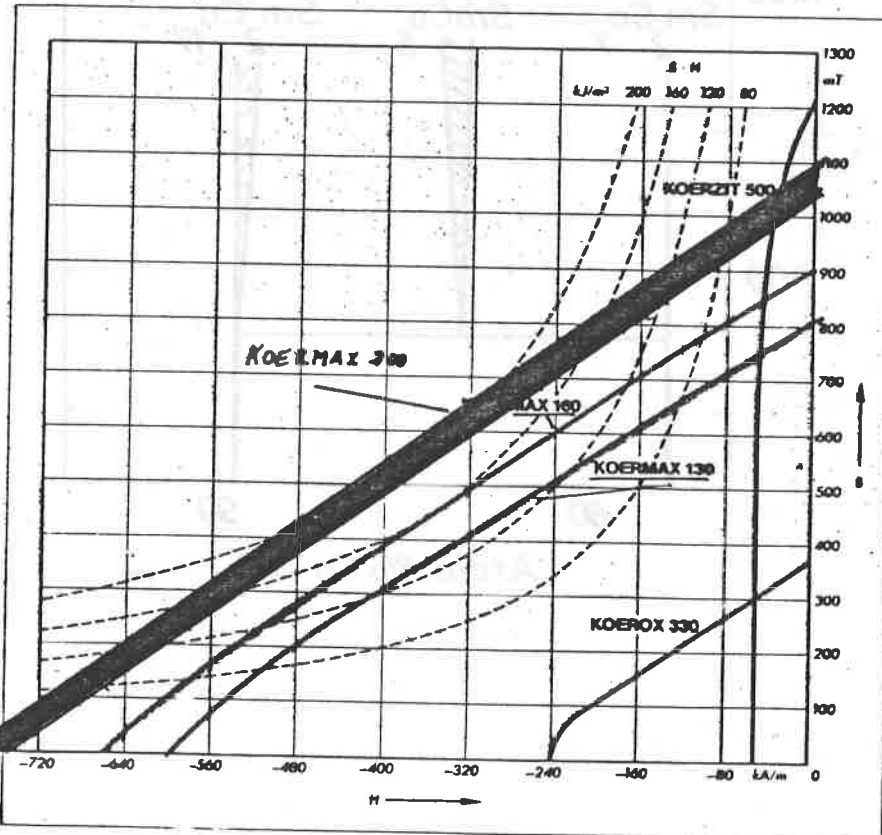
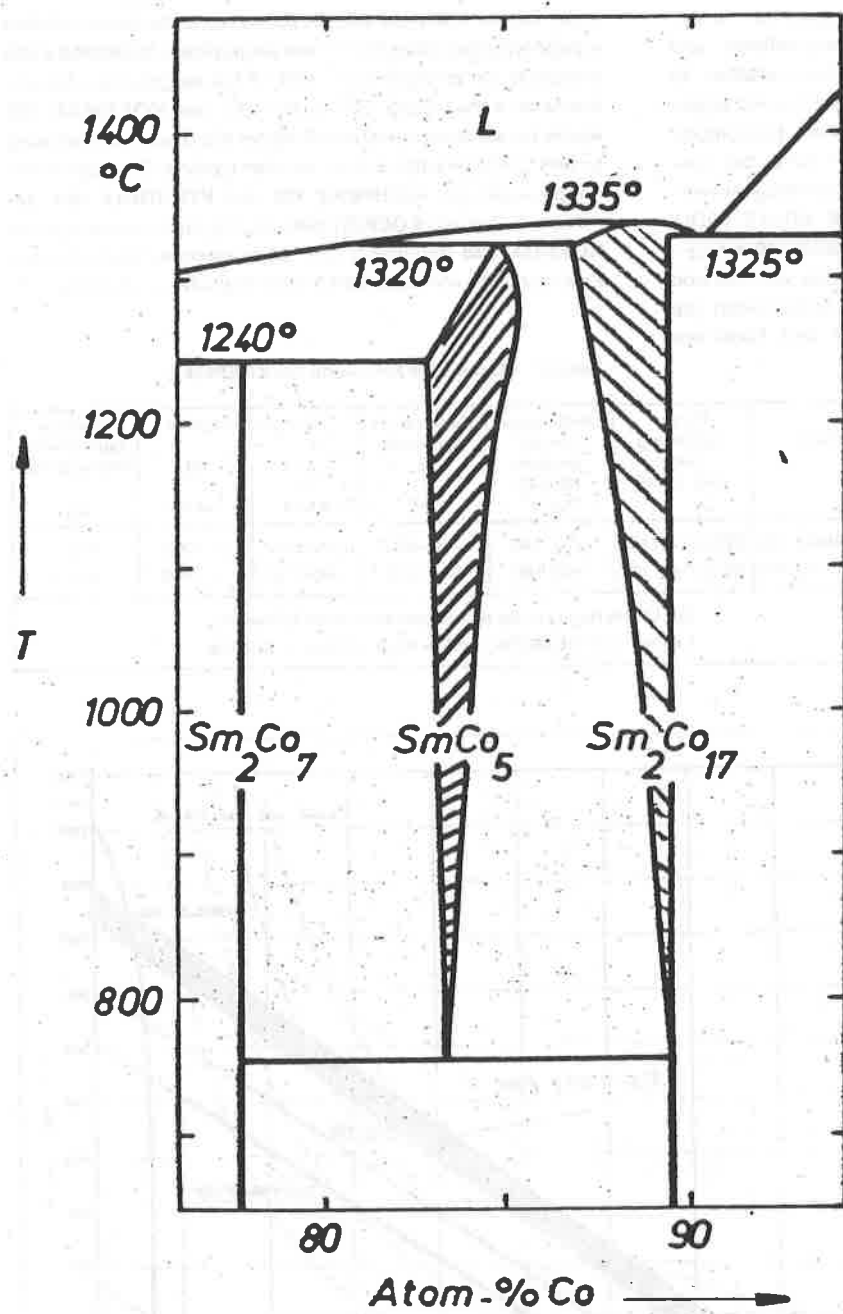
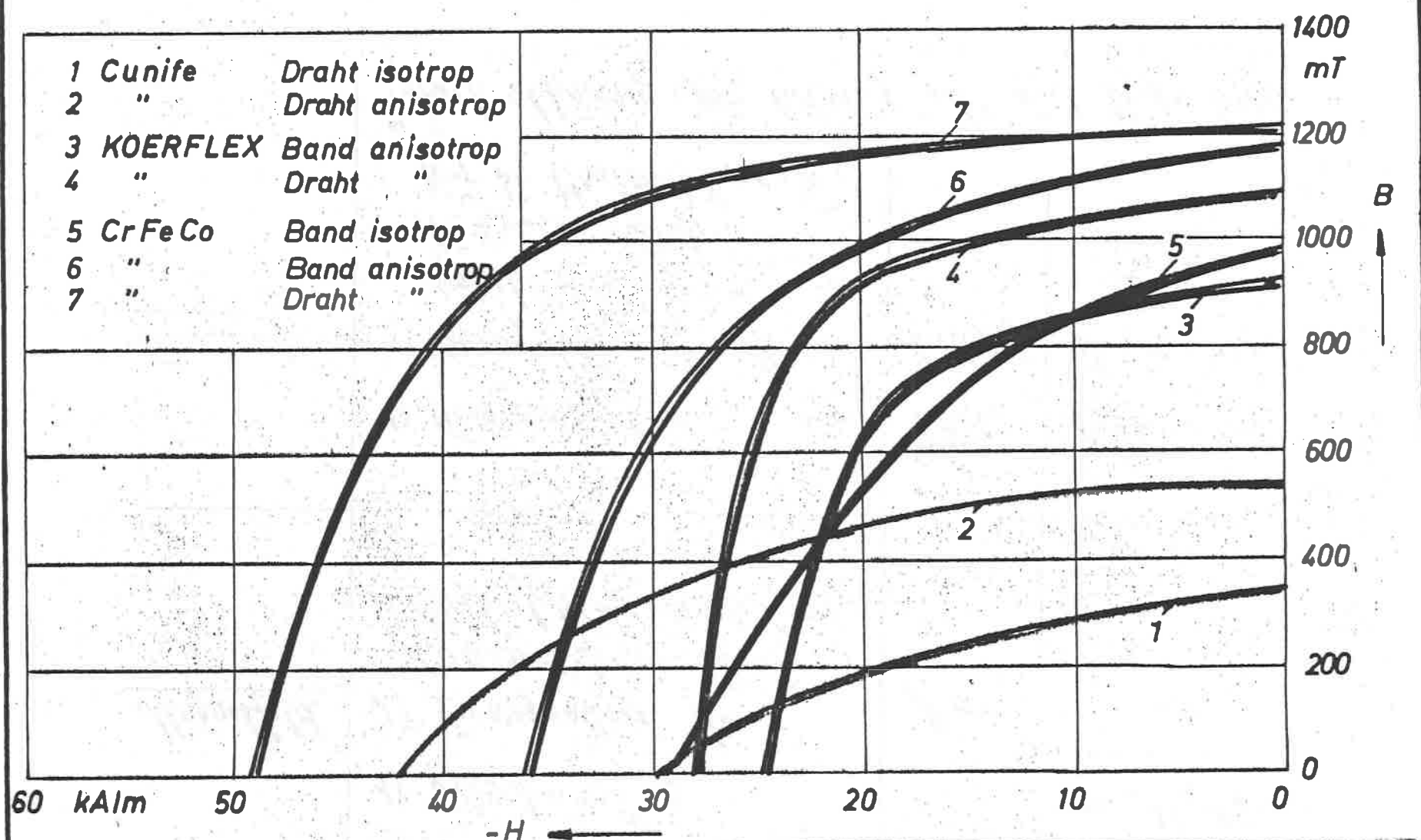


Bild 1: Typische Entmagnetisierungskurven von **KOERMAX 130** und **160**, **KOERZIT 500** und **KOEROX 330**

8





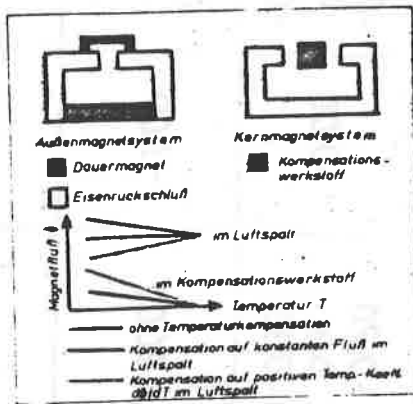

KRUPP WIDIA

Entmagnetisierungskurven verformbarer
Dauermagnete

MAGNET-
WERKSTOFFE

<u>Einflussgröße</u>	<u>Wirkungsweise^{a)}</u>	<u>Reaktion</u>
<u>Magnetfeld.</u>	1) Abschirmung 2) Verzögern der Ausbreitung durch Wechselfeld (Resistivität)	Nur 1)
<u>Temperatur</u>	1) Temperaturfeld 2) Verzögern der Aus- breitung durch die Abzählung (Stabilität). Nur bei Maximalkapazität	TK(0) TK(0)
	* stark abhängig von Arbeitpunkt und Vorgeschichte	(0)

— 6 —



$$\frac{\partial B_M}{\partial T} \cdot A_M = \frac{\partial B_L}{\partial T} \cdot A_L + \frac{\partial B_K}{\partial T} \cdot A_K$$

ES SOLL SEIN: $\frac{\partial B_L}{\partial T} = 0$

DARAUS FOLGT:

$$\frac{\partial B_M}{\partial T} \cdot A_M = \frac{\partial B_K}{\partial T} \cdot A_K$$

FORDERUNGEN AN EINEN TEMPERATURKOMPENSATIONSWERKSTOFF:

1. GEEIGNETE CURIETEMPERATUR

2. GROSSES $\frac{\partial B_K}{\partial T}$

THERMOPERM: $\frac{\partial B_K}{\partial T} = 7 \text{ mT/K}$

Mn-Zn-FERRIT: $\frac{\partial B_K}{\partial T} = 3 \text{ mT/K}$

	KOERZIT	KOEROX	KOERFLEX	KOERMAX	$\text{Sm}_2\text{Co}_{17}$	CrFeCo	MnAlC
Curietemperatur T_c °C	700-900	450	700	710	800-900	620-680	300-330
$\text{TK}(J_s)$ %/K 0-100 °C	-0,02	-0,20	-0,01	-0,04	-0,03	-0,03 bis -0,05	-0,10
$\text{TK}(H_c)$ %/K 0-100 °C	+0,03 bis -0,07	+0,20 bis +0,50	~0	-0,3	-0,20 bis -0,30	-0,09	-0,15 bis -0,20
Max. Einsatz- temperatur T °C	~500	~300	500	~250	(-200)	-500	(100 bis 150)
Gefügeinstabi- lität bei T °C	550	1100	520	250	(250)	510	530



KRÜPP WIDIA

Temperaturdaten verschiedener Dauermagnetwerkstoffe

MAGNET-
WERKSTOFFE



Für Dauermagnete relevante Normen

Gebiet	Bundesrepublik	International
Werkstoffe	DIN 17 410 (5/77)	IEC 68(CO)7 (8/75)
Bauformen	DIN 42 026/1 (9/77)	-
Magn. Messungen	DIN 50 470 (E 12/75) DIN 50 471 (3/71)	IEC 68(CO)12 (1/77)
Begriffe, Einheiten	DIN 1325 (1/72) DIN 1339 (11/71)	ISO 1000 (73) IEC Röbl. 50(901) (73) " " 50(901A)(75)

(\bar{w})

The permanent magnet circuit

1. Materials

2. Design

2.1. Methods

2.1.1. Conventional

2.1.2. Analytical

2.1.3. Numerical

2.2. Example (Core magnet assembly)

2.2.1. Conventional

2.2.2. Analytical

2.2.3. Numerical

3. Applications

1. Conventional method employed for the design of magnet assemblies

Combining the equations of
magnetic flux/magnetomotive force
for the magnet assembly.

$$\oint \mathcal{B} d\alpha = 0$$

$$\oint f d\mathcal{B} = 0$$

Results: Load line; operating point;
air gap flux density.

Problems: Evaluation of leakage factor;
accuracy of results.

Advantages: No computer program and no
mathematical experience needed.

Fried. Krupp GmbH **KFI** Krupp Forschungsinstitut

Magnetostatic circuit

$$\oint \mathbf{B} d\alpha = 0 \rightarrow B_m A_m = B_g A_g + B_e A_e = \sigma B_g A_g$$

$\sigma > 1$: leakage factor ($\sigma \sim ?$)

$$\oint \mathbf{H} d\mathbf{l} = 0 \rightarrow -H_m l_m = H_g l_g + H_{Fe} l_{Fe} = \gamma H_g l_g$$

$\gamma > 1$: Mmf - factor ($\gamma \sim 1,15$)

$$\text{Air gap energy: } \frac{1}{2} \mu_0 H_g^2 = \frac{1}{2} \cdot \frac{(B_m H_m)}{\sigma \gamma} V_m$$

$$\text{Load line: } \frac{B_m}{-\mu_0 H_m} = \frac{\sigma A_g l_m}{\gamma A_m l_g}$$

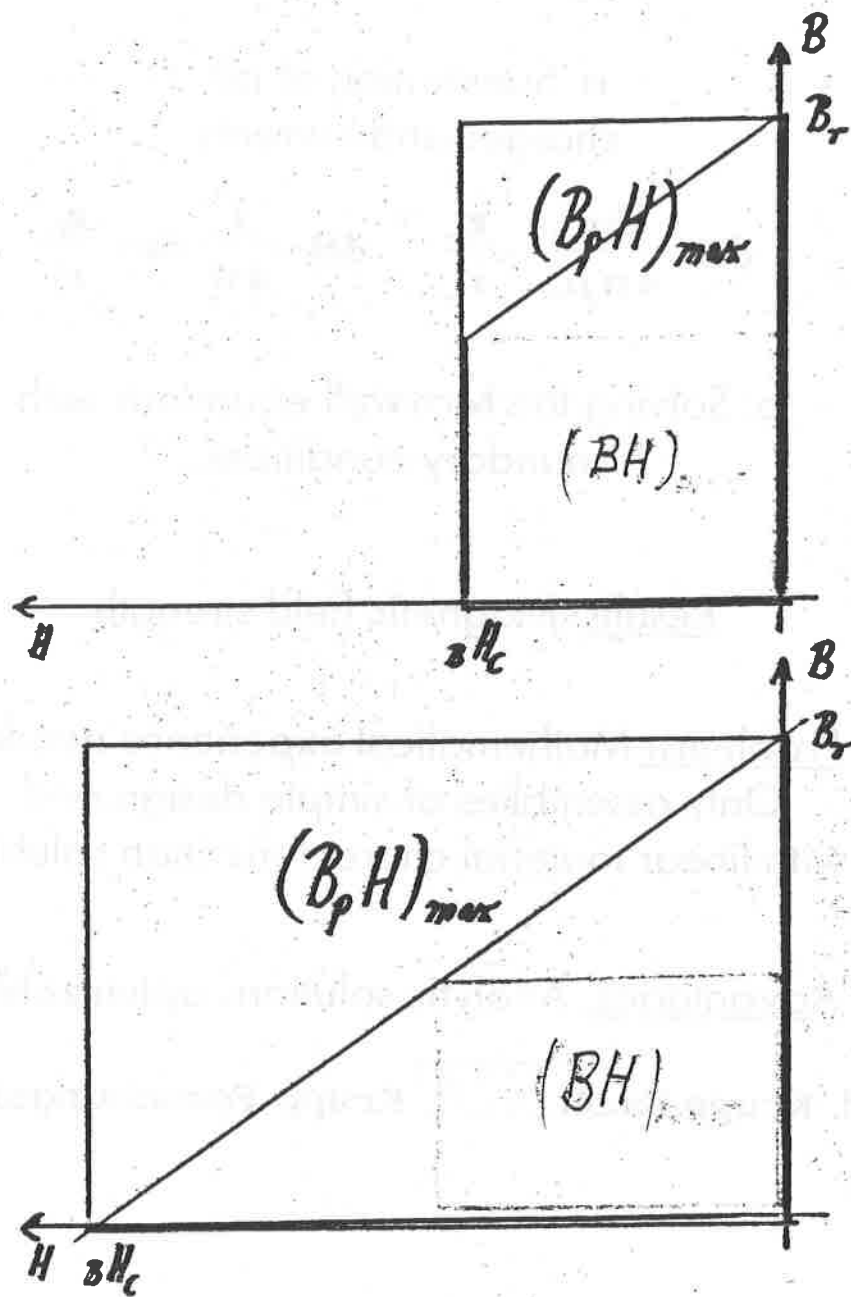
$$\text{Demagnetization curve: } B = B(H)$$

Working point $(B_m; H_m)$: Intersection of
load line and demagnetization curve

$$\oint \mathbf{H} dl = n$$

17

$(BH)_{\max}$ and $(B_p H)_{\max}$



2. Analytical methods employed for the design of magnet assemblies.

a. Summation of all charges and currents:

$$d\mathbf{H} = \frac{dm}{4\pi\mu_0} \cdot \frac{\mathbf{r}_0}{r^2} \quad d\mathbf{H} = \frac{I}{4\pi} ds \times \frac{\mathbf{r}_0}{r^2}$$

b. Solving the Maxwell equations with boundary conditions.

Results: Magnetic field strength

Problems: Mathematical experience needed;
Only assemblies of simple design and with linear material characterization soluble.

Advantages: Analytic solutions optimizable.

Fried. Krupp GmbH **KFI** Krupp Forschungsinstitut

3. Numerical methods employed for the design of magnet assemblies.

a. Summation method.

Summation of all charges and currents.

Problems: Iteration for linear material characterization.

Advantages: Only subdivision of magnetic materials/coils

b. Finite difference method.

Change from differential to difference equations.

Problems: Boundary conditions; interfaces.

c. Finite element method.

Minimizing the energy/calculus of variation.

Results: Magnetic field strength (a);
Scalar or vector potential (b),(c).

Problems: Computer/computer program needed;
Optimizing by repeated calculations.

Advantages: Each problem soluble.

Finite element method

Total energy = $f(\text{potential}) = \text{Minimum.}$

Total energy = $\sum_{\text{Finite elements}} \text{Energy.}$

Energy = $f(\text{potentials in the nodes}).$

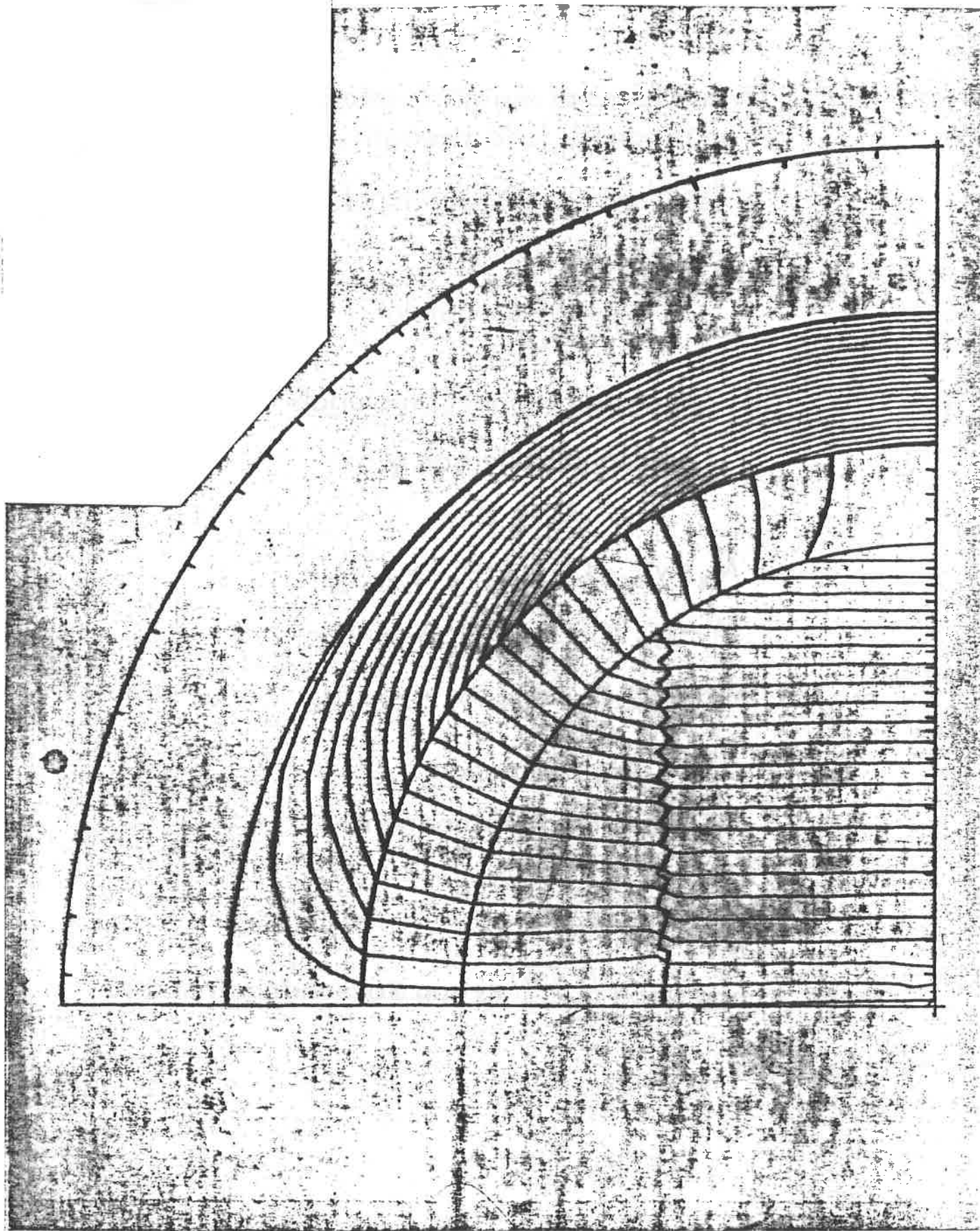
$\frac{\partial \text{total energy}}{\partial \text{node potentials}} = 0 \Rightarrow \text{System of equations.}$

Number of nodes = Number of unknowns.

- 1.step: Generating the grid;
- 2.step: Setting up and solving the system of equations;
- 3.step: Computing the magnetic field strength H;
- 4.step: Only for nonlinear material characterization:
Input of new material data according to H.

- 5.step: Compare 2.step
 - 6.step: Compare 3.step
 - 7.step: Compare 4.step
- } Iteration

Fried. Krupp GmbH **KFI** Krupp Forschungsinstitut



Dependence of magnetization on magnetic field strength

a) Isotropic magnetic material:

Susceptibility χ

$$\mathbf{M} = \chi \cdot \mathbf{H} : \text{Measurement}$$

b) Anisotropic magnetic material:

Susceptibility tensor χ

$$\mathbf{M} = \chi \cdot \mathbf{H}$$

$$M_x = \chi_{xx} \cdot H_x + \chi_{xy} \cdot H_y + \chi_{xz} \cdot H_z$$

$$M_y = \chi_{yx} \cdot H_x + \chi_{yy} \cdot H_y + \chi_{yz} \cdot H_z$$

$$M_z = \chi_{zx} \cdot H_x + \chi_{zy} \cdot H_y + \chi_{zz} \cdot H_z$$

Approximation:

$$M_x \approx \chi_{xx} \cdot H_x : \text{Measurement}$$

$$M_y \approx 0$$

$$M_z \approx 0$$

Abstract:

Using the example of a core magnet system, consisting of a diametrically magnetized cylindrical magnet and a concentric magnetically soft magnetic return path, the three commonly used methods for computing permanent magnet systems are outlined.

The advantages and disadvantages of the conventional methods, analytic and numerical computation, are described with mention of their scope and limitations.

Fried. Krupp GmbH **KFI** Krupp Forschungsinstitut

Conventional design method

Magnetomotive force: $\tau \cdot H_m L_m = -H_g L_g ; \tau \approx 0,85$

Flux relation: $\sigma \cdot B_m A_m = \mu_0 H_g A_g ; \sigma \leq 1,00$

Load line:
$$\frac{B_m}{\mu_0 H_m} = \frac{\tau}{\sigma} \frac{A_g}{A_m} \frac{L_m}{L_g}$$

Gap energy: $\mu_0 H_g^2 V_g = \tau \cdot \sigma |B_m H_m| \cdot V_m$

$$L_m = \frac{\pi}{4D} (D^2 - d^2) ; A_m = (D - d) \cdot h$$

$$L_g = D_{Fe} - D ; A_g = \frac{\pi h}{4} (D_{Fe} + D)$$

|| $D_{Fe} = 20 \text{ mm}; D = 16 \text{ mm}; d = 3,8(0,0) \text{ mm}$

|| $h = \infty \Rightarrow \sigma = 1,00 ; \tau = 0,85$

|| $B_r = 920 \text{ mT}; \mu_p = 1,00$

$B_m / (-\mu_0 H_m) = 5,84 (4,72)$

$H_m = -108 (128) \text{ kA/m}; B_m = 793 (759) \text{ mT}$

Fried. Krupp GmbH **KFI** Krupp Forschungsinstitut

$A_m = (D - d) \cdot h$ ist sicherlich falsch

$A_m = D \cdot h$ ist sicherlich besser

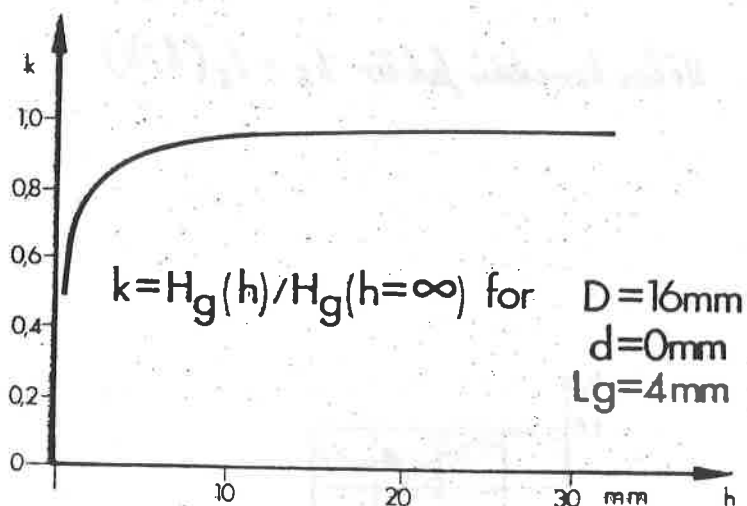
So ist $\frac{L_m}{A_m} = \frac{\pi}{4D} \frac{(D-d)(D+d)}{(D-d) \cdot h} = \frac{\pi(D+d)}{4Dh} \left| \begin{array}{c} \frac{\pi}{4} \\ \frac{D+d}{h} \end{array} \right|$

$$H_g = \frac{\hat{H}_g}{\pi/2} \cdot \int_0^{\pi/2} \sin\varphi \cdot d\varphi ; \quad \hat{H}_g = \frac{\pi}{2} \cdot H_g$$

$$H_g = 272(342) \text{ kA/m} ; \quad \hat{H}_g = 427(537) \text{ kA/m}$$

Analytically computed: $H_r(9\text{mm}; 90^\circ) = 494(524) \text{ kA/m}$

Reduction of H_g ($h=\infty$) for finite h :



Fried. Krupp GmbH **KFI** Krupp Forschungsinstitut

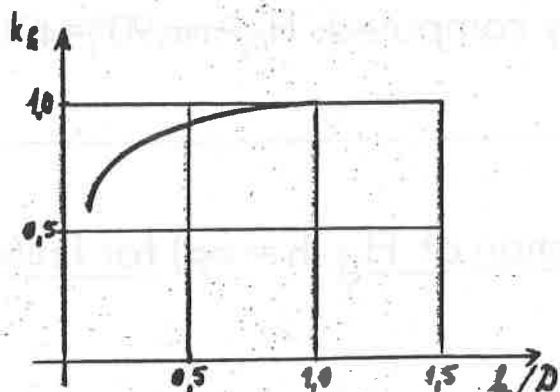
Die Flüsse Φ_N, Φ_{STR} sind proportional
 den Verhältnissen der Nenn-Höhe und des
 Leitfächters $R = \frac{L}{\mu_0(\mu_r) A} + \frac{1}{R} = \frac{\mu_0(\mu_r) h}{L}$

$$D = 16 \text{ mm}$$

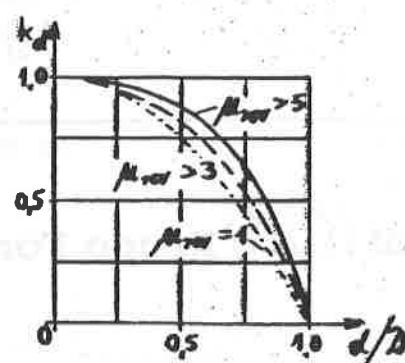
$$l = 2 \text{ mm}$$

26

$$H'_e(l, d) = H_e(l = \infty, d = 0) \cdot k_e \cdot k_d$$

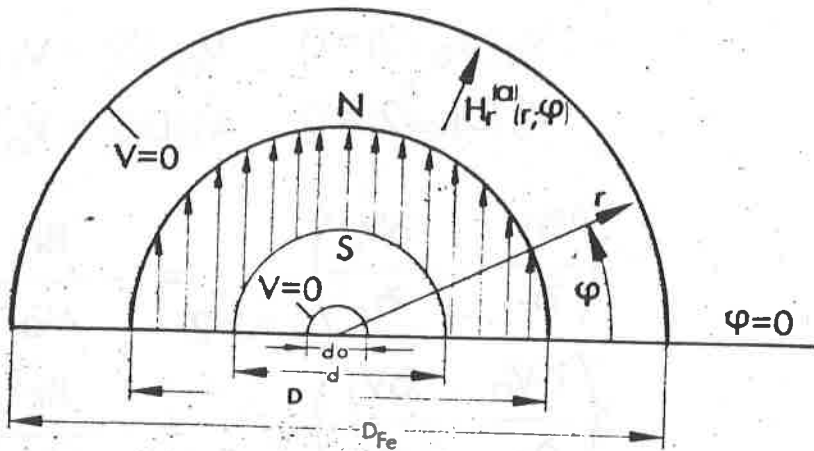


$$\text{Höhenkorrekturfaktor } k_e = k_e(l/D)$$



$$\text{Lockkorrekturfaktor } k_d = k_d(d/D)$$

Analytical solution



Assumptions:

Permanent magnetic material with $\mu_p \approx 1$ (fixed magnetization).

Soft magnetic material with $\mu_r \gg 1$ ($\mu_r = \infty$)

Laplace equation:

$$\Delta V = \frac{\partial^2 V}{\partial r^2} + \frac{1}{r} \cdot \frac{\partial V}{\partial r} + \frac{1}{r^2} \cdot \frac{\partial^2 V}{\partial \varphi^2} = 0$$

Ansatz:

$$V_O = (V_O^+ \cdot r + V_O^- \cdot r^{-1}) \cdot \sin \varphi \quad d_o \leq 2r \leq d$$

$$V_i = (V_i^+ \cdot r + V_i^- \cdot r^{-1}) \cdot \sin \varphi \quad d \leq 2r \leq D$$

$$V_a = (V_a^+ \cdot r + V_a^- \cdot r^{-1}) \cdot \sin \varphi \quad D \leq 2r \leq D_{Fe}$$

Boundary conditions:

$$V_O(d_O/2) = 0 \quad V_O(d/2) = V_i(d/2)$$

$$V_a(D_{Fe}/2) = 0 \quad V_i(D/2) = V_a(D/2)$$

$$\left(\frac{\partial V_i}{\partial r} - \frac{\partial V_O}{\partial r} \right)_{r=d/2} = - \frac{Br}{\mu_0} \cdot \sin\varphi$$

$$\left(\frac{\partial V_a}{\partial r} - \frac{\partial V_i}{\partial r} \right)_{r=D/2} = \frac{Br}{\mu_0} \cdot \sin\varphi$$

Solutions:Bore without iron:

$$H_r^{(a)}(r; \varphi) = \frac{Br}{2\mu_0} \cdot \frac{D^2 - d^2}{D_{Fe}^2} \cdot \left\{ 1 + \left(\frac{D_{Fe}}{2r} \right)^2 \right\} \cdot \sin\varphi$$

Bore filled with iron ($d = d_O$):

$$H_r^{(a)}(r; \varphi) = \frac{Br}{2\mu_0} \cdot \frac{D^2 - d^2}{D_{Fe}^2 - d^2} \cdot \left\{ 1 + \left(\frac{D_{Fe}}{2r} \right)^2 \right\} \cdot \sin\varphi$$

Effect of iron in the bore:

$$\frac{H_r^{(a)}(\text{with iron}) - H_r^{(a)}(\text{without iron})}{H_r^{(a)}(\text{without iron})} = \frac{1}{(D_{Fe}/d)^2 - 1}$$

Feldstärke im Lüftspalt

$$H_r(r_i, \varphi) = \frac{B_r}{2\mu_0} \cdot \frac{D^2 - d^2}{u_a^+ D_{Fe}^2 - u_i^- d^2} \cdot \left\{ 1 + u_a^+ \left(\frac{D_{Fe}}{2r} \right)^2 \right\} \cdot \sin \varphi$$

$$H_\varphi(r_i, \varphi) = \frac{B_r}{2\mu_0} \cdot \frac{D^2 - d^2}{u_a^+ D_{Fe}^2 - u_i^- d^2} \cdot \left\{ 1 - u_a^+ \left(\frac{D_{Fe}}{2r} \right)^2 \right\} \cdot \cos \varphi$$

$$u_a^+ = \frac{\mu_r^{(u)} + 1}{\mu_r^{(u)} - 1} \quad u_i^- = \frac{\mu_r^{(i)} - 1}{\mu_r^{(i)} + 1}$$

$$= 1 \quad = 1$$

$$= \infty \quad = 0$$

für $\mu_r = \infty$

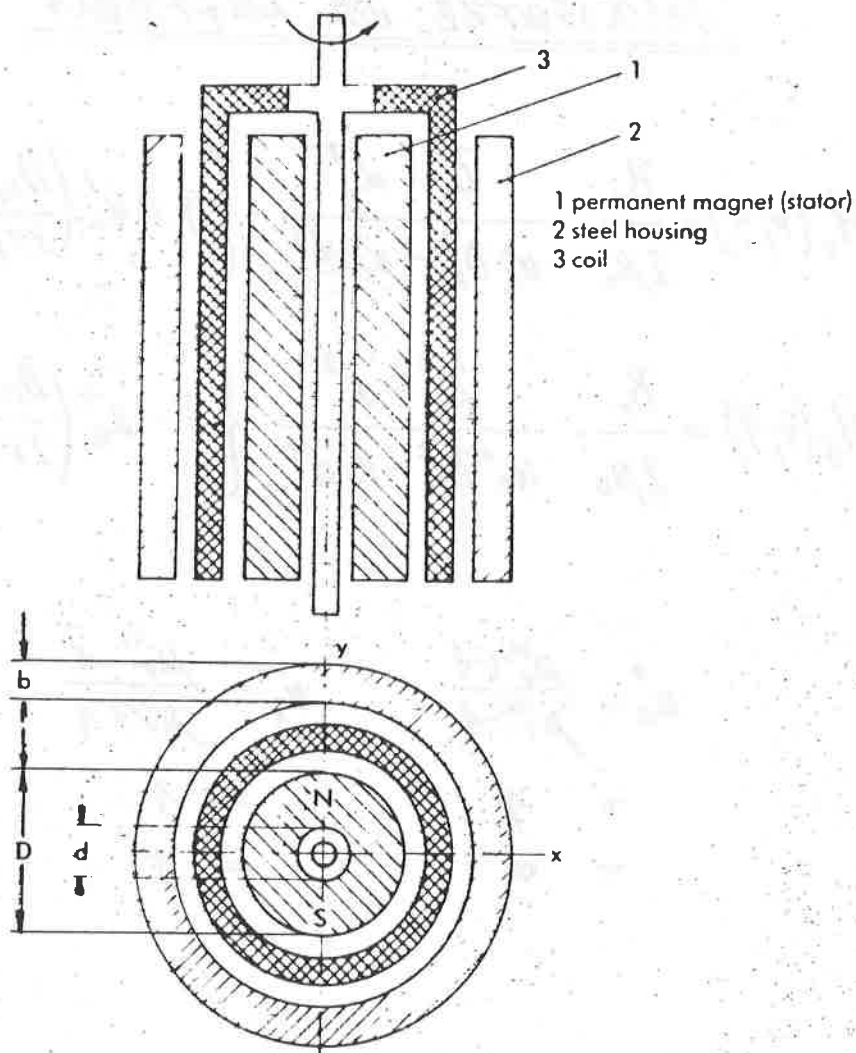
für $\mu_r = 1$

innen Luft $\mu_r^{(i)} = 1$

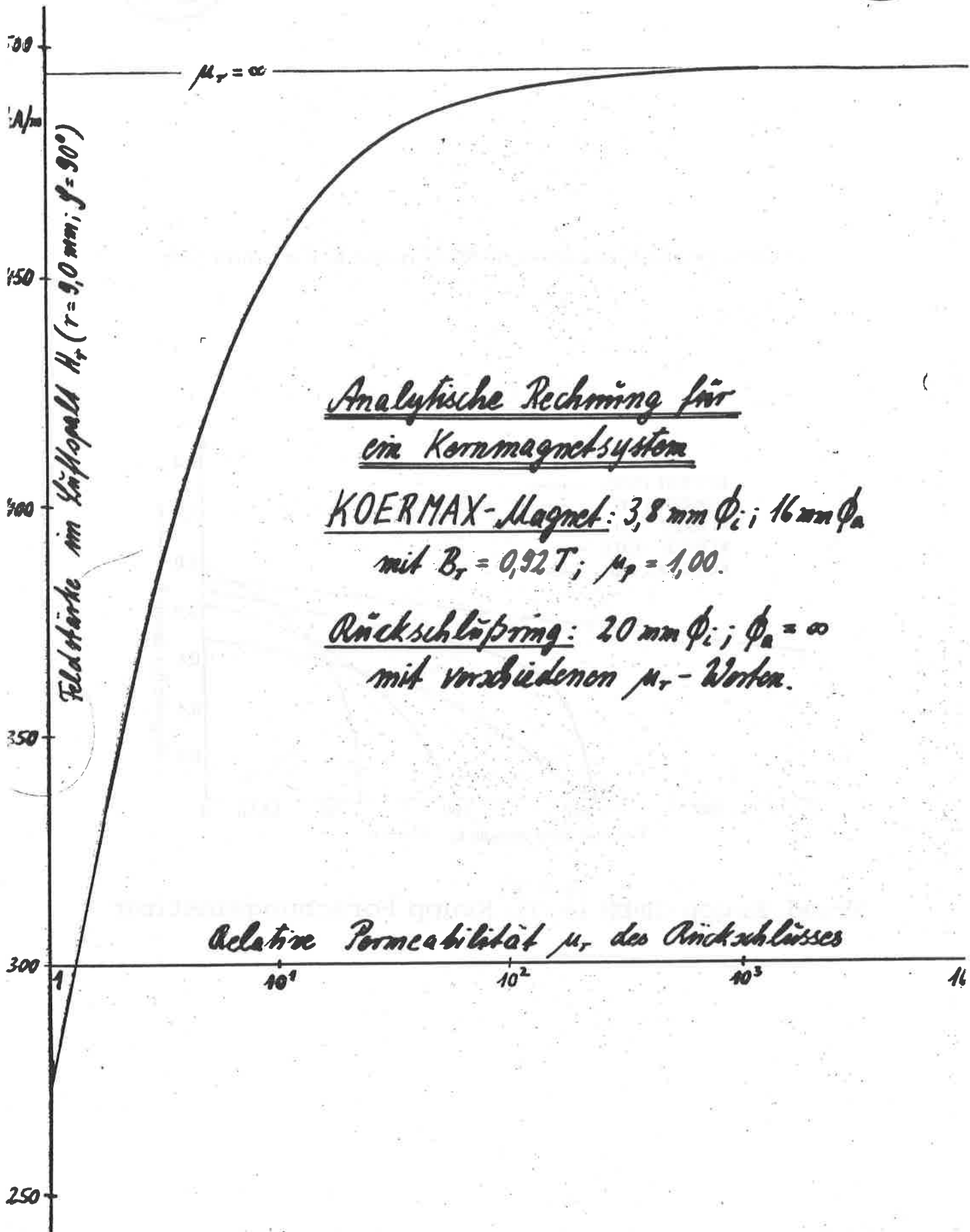
RESERVE

30

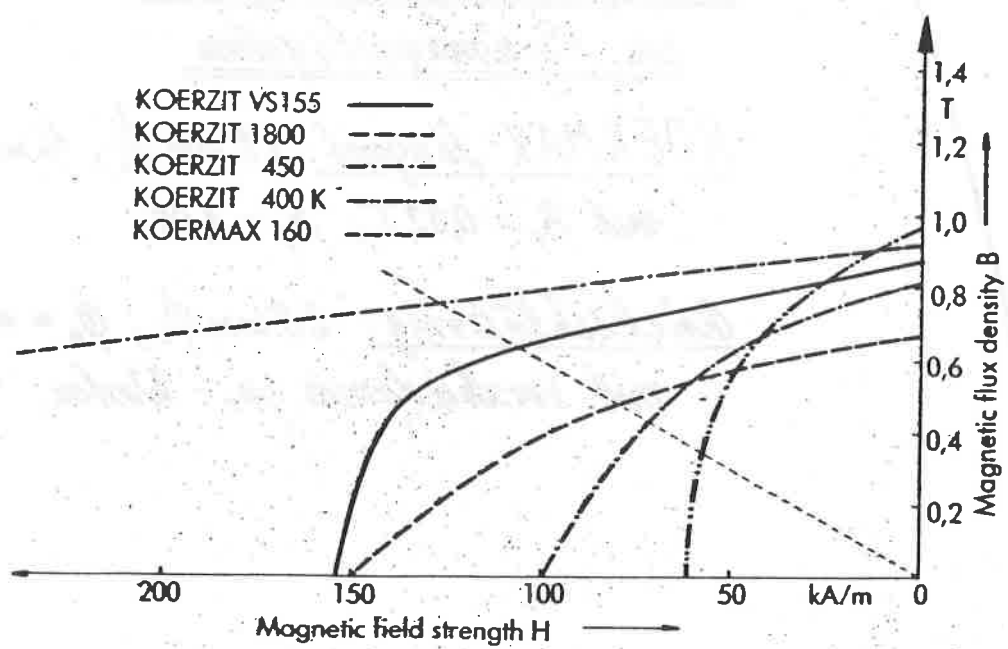
Moving-coil motor schematic cross-section



Fried. Krupp GmbH **KFI** Krupp Forschungsinstitut



Demagnetization curves of AlNiCo and RECo₅-materials



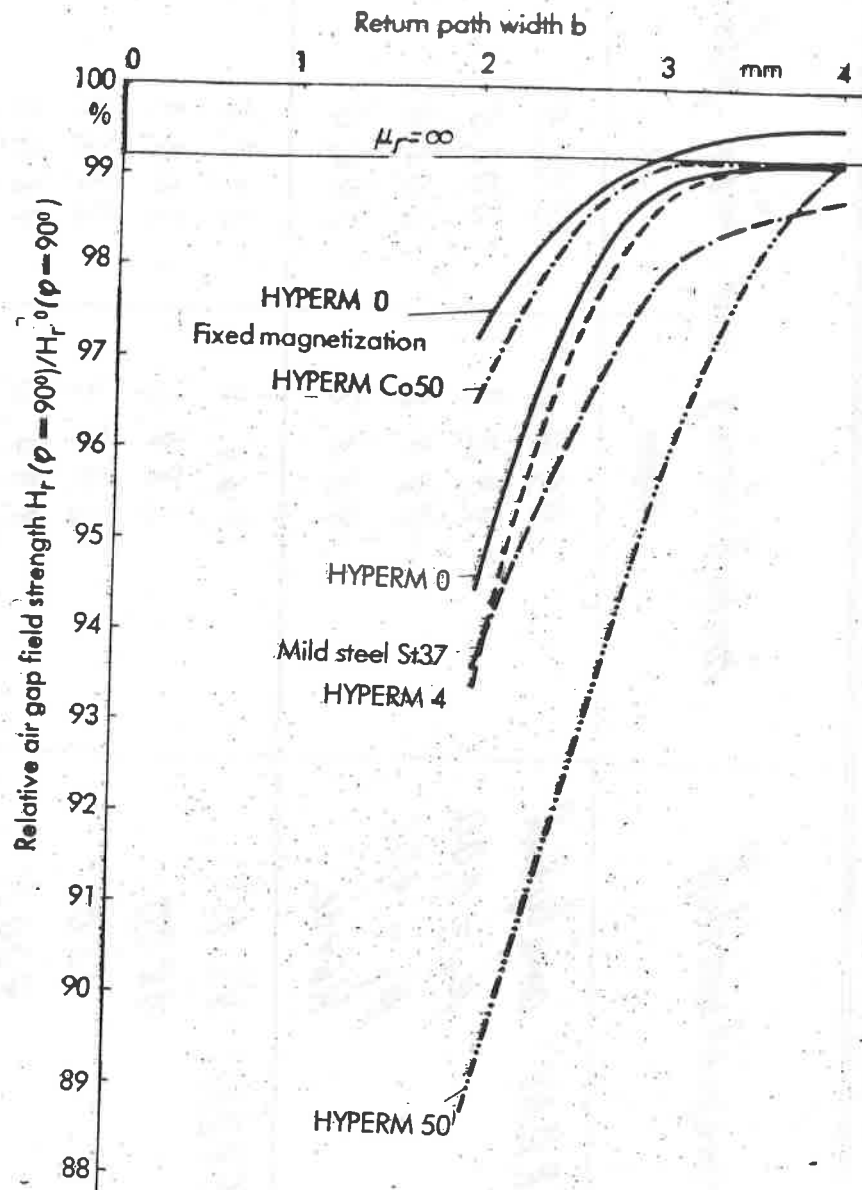
Fried. Krupp GmbH **KFI** Krupp Forschungsinstitut

Lüftspaltfeldstärke H_r ($r = 9\text{mm}$; $\vartheta = 90^\circ$) in kA/m

Dämmmagnetwerkstoff	Innenbohrung mit Eisen gefüllt	
	nom	ja
KOERMAX analytisch	494,0	512,5
$\mu_p = 1,00$	490,3	507,5
$\mu_p = 1,05$	484,8	502,4
Kürze	488,2	506,0
KOERZIT VS 155	366,9	398,4
1800	284,5	303,9
450	245,1	255,7
400K	194,0	187,2

(WW)

KOERMAX 160 core magnet system with various materials of the return path ring



Fried. Krupp GmbH **KFI** Krupp Forschungsinstitut

H_r^0 : Feldstärke im Außenring eines KOERMAX-Systems mit zumindest
Kernsteigung des KOERMAX und $\mu_r = \infty$ für ein festes Blech-
material.

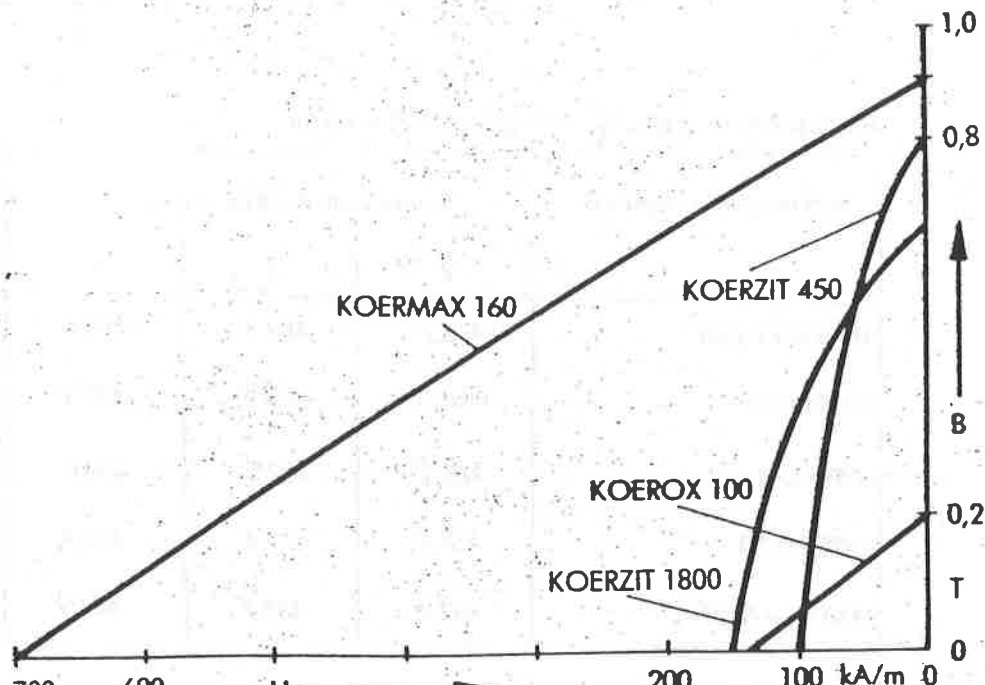
KOERMAX 160 core magnet system with various materials of the return path ring

Air gap field strength H_g ($r = 9 \text{ mm}$; $\vartheta = 90^\circ$) in kA/m

Soft magnetic material	Return path width b in mm		
	2	3	4
HYPERM Co50	476,7	489,8	490,0
HYPERM 0	466,3	488,7	489,8
HYPERM 4	461,3	487,5	490,0
HYPERM 50	437,9	472,4	489,9
Mild steel St 37	462,4	483,7	487,9

Fried. Krupp GmbH **KFI** Krupp Forschungsinstitut

**Demagnetization curves
for some permanent magnet materials**



Fried. Krupp GmbH **KFI** Krupp Forschungsinstitut

Permanent Magnet Systems

Advantages: No electrical energy required.
No heat evolved.
Constant magnetic flux density.

Disadvantages: Flux density limited.
Difficult to control.

Anwendungen

Magnetverschlüsse
Schalter

Sonden, Sensoren

Lautsprecher
Mikrofone

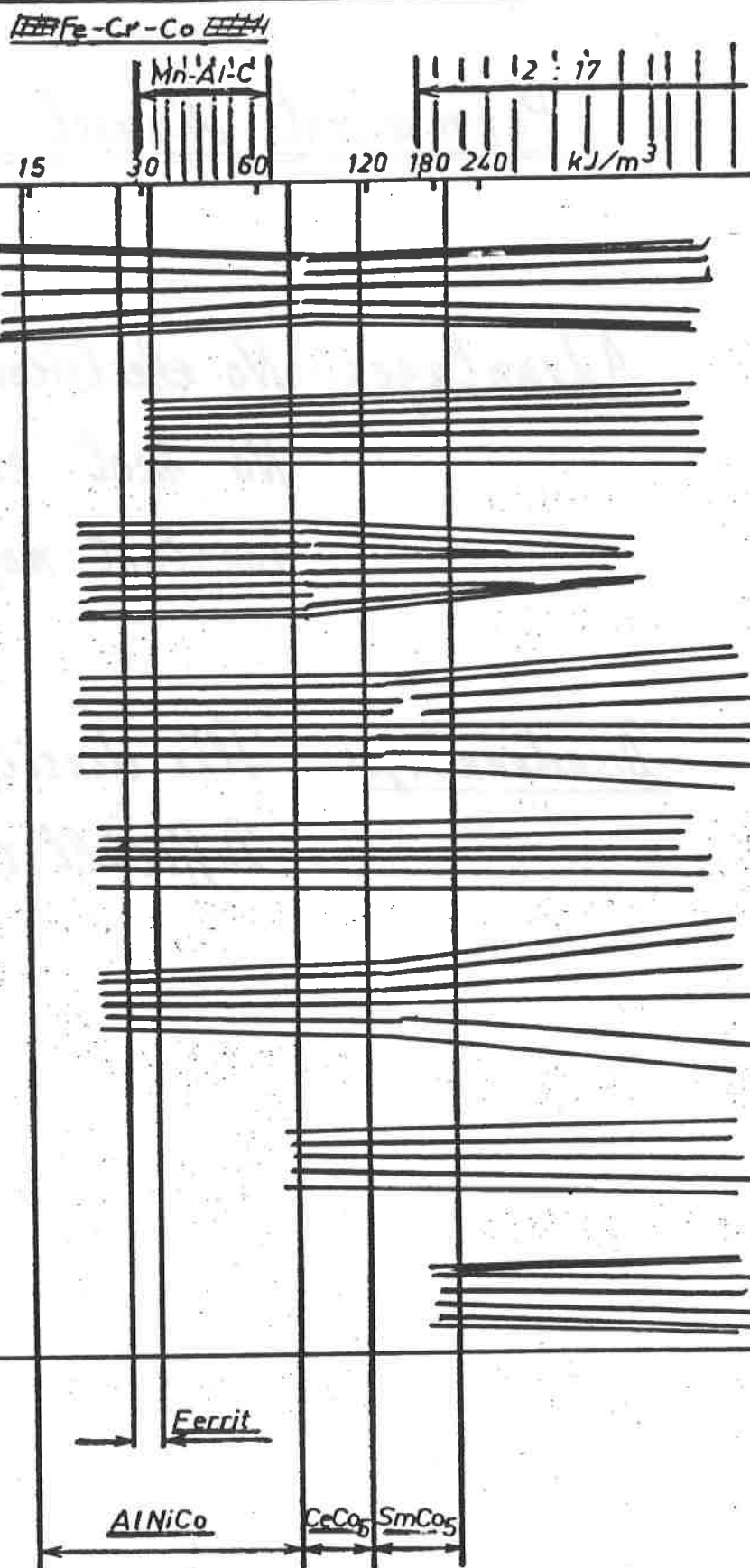
Motoren
Generatoren

Magnetscheider
Filter

Kupplungen
Lager

Mikrowellenröhren
Jonenoptik

Schwebetechnik



SWITCHABLE LIFTING MAGNET

**CONTROLLED BY TURNING
THE PERMANENT MAGNET**

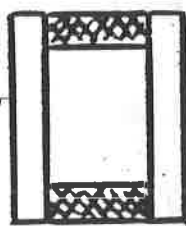
WEIGHT: 11 kg

MAXIMUM FORCE: 10 kN

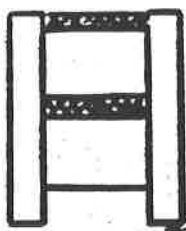
FORCE AT 1MM: 2 kN

CALCULATIONS: NUMERICAL

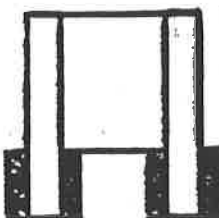
Switchable permanent magnet systems.



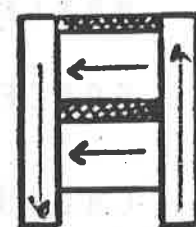
Demagnetizing



Magnetizing in the
opposite direction



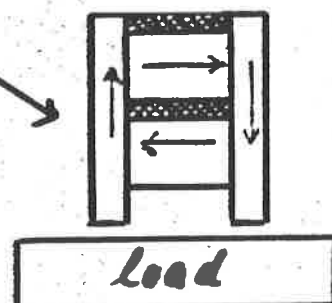
Compensating the flux



On



Off



41

COAXIAL SYNCHRONOUS COUPLING

NUMBER OF POLES: 120

AIR GAP: 2 MM

MAXIMUM TORQUE: 4 KN.M

CALCULATIONS: ANALYTICAL
NUMERICAL

42

COAXIAL SYNCHRONOUS COUPLING

TORQUE IN kN·M, NORMALIZED TO
A COUPLING LENGTH $A = 96 \text{ mm}$

MEAN POLE DISTANCE $B = 13.5 \text{ mm}$

	A IN MM	A/B	NUMBER OF BACK-CIRCUITS		
			2	1	0
ANALYTICAL	10	0.75	2.88	2.25	1.81
"	96	7.1	4.53	3.44	2.60
"	00	00	4.64	3.49	2.62
NUMERICAL	00	00	4.615	3.412	2.582
MEASURED	96	7.1	4.65	-	-

RADIAL MAGNETIC BEARING

AXIALLY MAGNETIZED CONCENTRIC
RINGS WITHOUT IRON

AIR GAP: 2 MM

RADIAL STIFFNESS: 22 MN/M

CALCULATIONS: ANALYTICAL WITH
NUMERICAL INTEGRATION

LIMITING VALUES OF MAGNETIC FORCES

ATTRACTION OR REPULSION WITH PERMANENT MAGNETS

ATTRACTION WITH SOFT MAGNETIC MATERIALS

M·A·K

K → 1

SHEAR FORCE

M·A·K

K → 0.75

TORQUE

M·A·K·R

K → 0.75

RADIAL BEARING

M·A·K

K → 0.32

MATERIAL FACTOR

$$M = \frac{B^2}{R/2l_0}$$

AREA OF AIR GAP

A

MEAN RADIUS OF AIR GAP

R

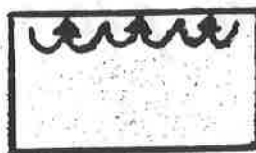
GEOMETRIC FACTOR

K

Magnetic fields with permanent magnets

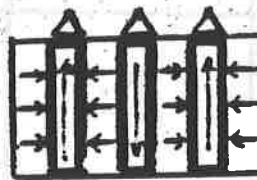
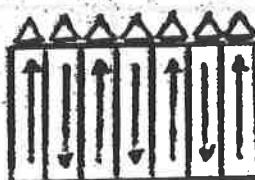
Methods

1. Without soft magnetic material



in isotropic water. with "blocking" magnets

2. With soft magnetic material



with pole-pieces

with pole-pieces

Magnetic fields with permanent magnets

Maximum field values

		Pole-pieces			
		without	with		
		only PM	with SM	only PM	with SM
Plane surface		$B_r/2$	$J_s/2$	∞	∞
air gap		B_r	J_s	∞	-

Remanence of permanent magnet

material (PM) : B_r

Saturation of soft magnetic

material (SM) : J_s

47

COMPUTATIONAL METHOD

ASSUMPTION: FIXED MAGNETIZATION

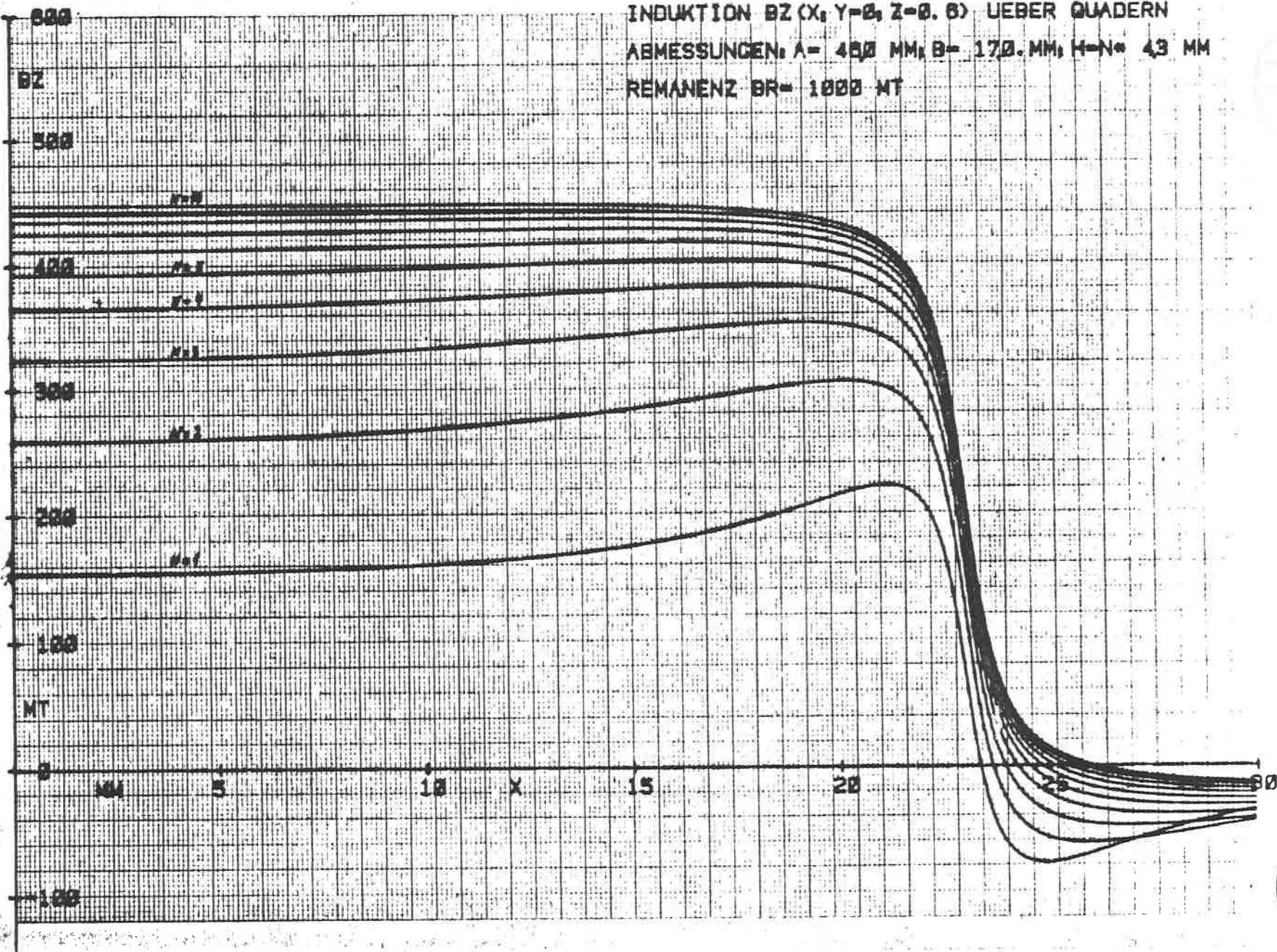
FLUX DENSITY OF A BAR MAGNET:

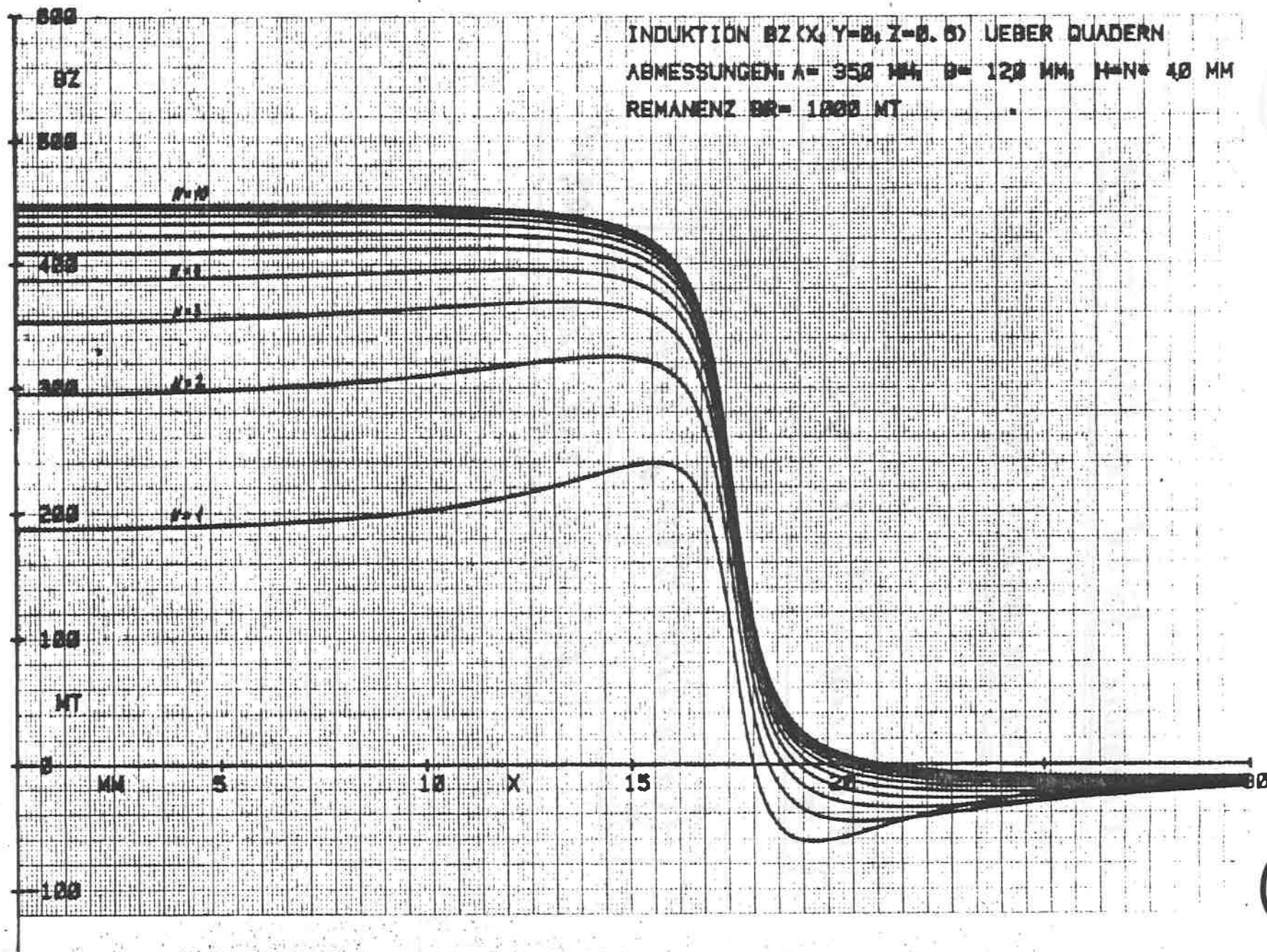
$$B_z(x, y, z) = \frac{J_R}{4\pi} \operatorname{ARCTAN} \left(\frac{(x-x') \cdot (y-y')}{(z-z') \cdot s} \right) \begin{vmatrix} +A & +B & +H \\ -A & -B & -H \end{vmatrix}$$

$$B_x(x, y, z) = \frac{J_R}{4\pi} \ln \left(\frac{(y-y')+s}{(z-z')+s} \right) \begin{vmatrix} +A & +B & +H \\ -A & -B & -H \end{vmatrix}$$

$$B_y(x, y, z) = \frac{J_R}{4\pi} \ln \left(\frac{(x-x')+s}{(z-z')+s} \right) \begin{vmatrix} +A & +B & +H \\ -A & -B & -H \end{vmatrix}$$

$$s = ((x-x')^2 + (y-y')^2 + (z-z')^2)^{1/2}$$





46

Magnetic field in the air gap
of permanent magnet systems

$$H_{\downarrow}(r=0; z=0) = J \left\{ 1 - \frac{1}{\sqrt{1 + (r_0/z_2)^2}} \right\}.$$

$$H_{\downarrow}(r=0; z=0) = 0.886 J \cdot l_2(z_1/z_2)$$

for $z_0 = 0$ and $2\alpha = 109,5^\circ$

51

PERMANENT HEXAPOLE MAGNET

COMPOSED OF

6 RARE EARTH COBALT BARS

MAGNETIC REMANENZ

910 MT

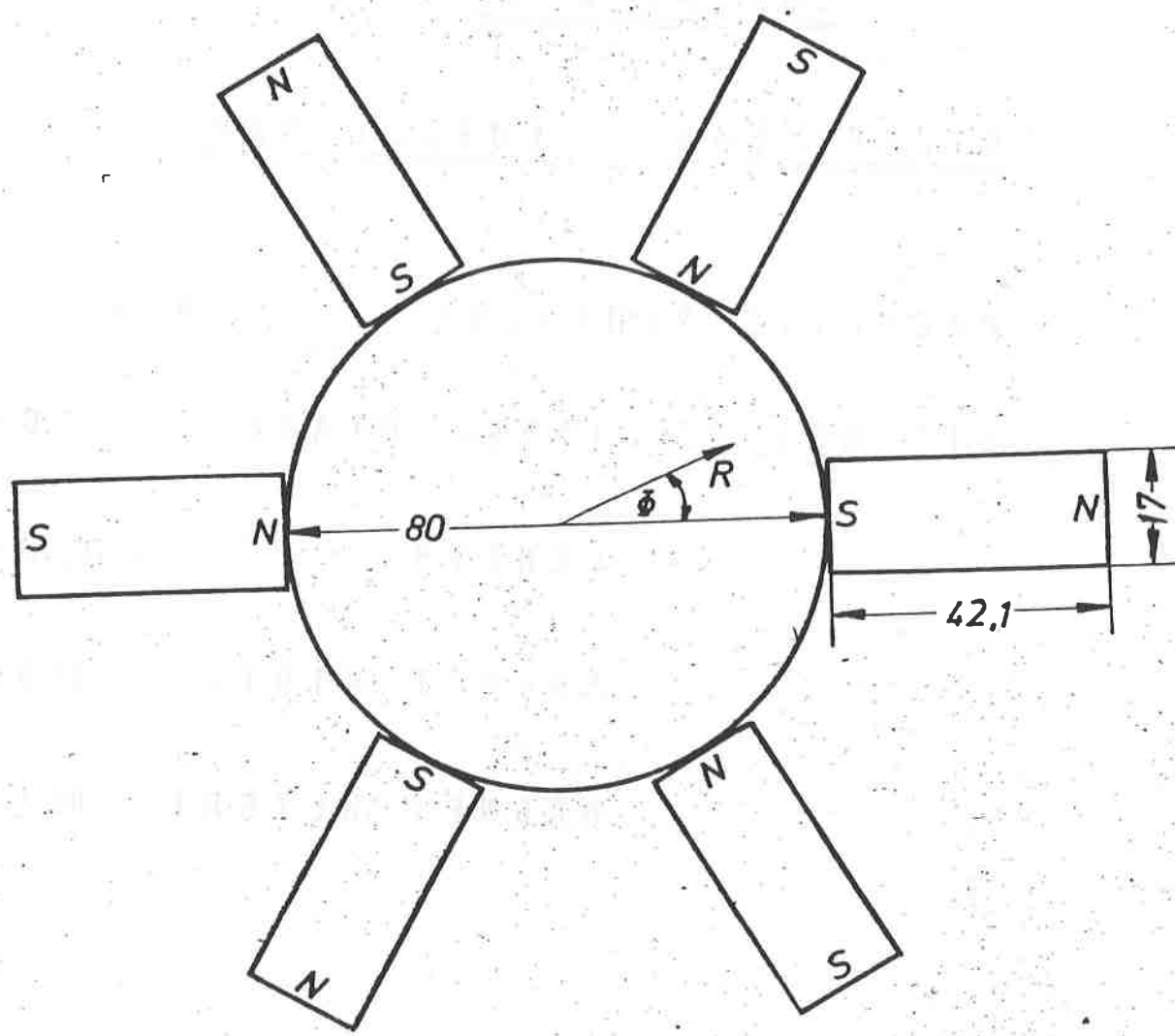
DIMENSIONS: INNER DIAMETER 80.0 MM

LENGTH

700.0 MM

MAGNET WIDTH 17.0 MM

MAGNET HEIGHT 42.1 MM



PERMANENT HEXAPOLAR MAGNET
CROSS SECTION

(C1
W)

800

B

700

600

500

400

300

200

100

MT

BETRAG DER INDUKTION B EINES HEXAPOLIS.

INNENRADIUS RL = 40.0001 MM

POLBREITE B = 17 MM

MAGNETHOEHE H = 42.1 MM

LAENGE DES HEXAPOLIS L = 700 MM

REMANENZINDUKTION BR = 910 MT

PERMANENT HEXAPOLAR MAGNET

INDUCTION IB(R,ΦZ)

 $\Phi_x 0^\circ : R$

40mm

35mm

 $\Phi = 30^\circ : R$

35mm

25mm

40mm

25mm

15mm

15mm

MM 50

100

150

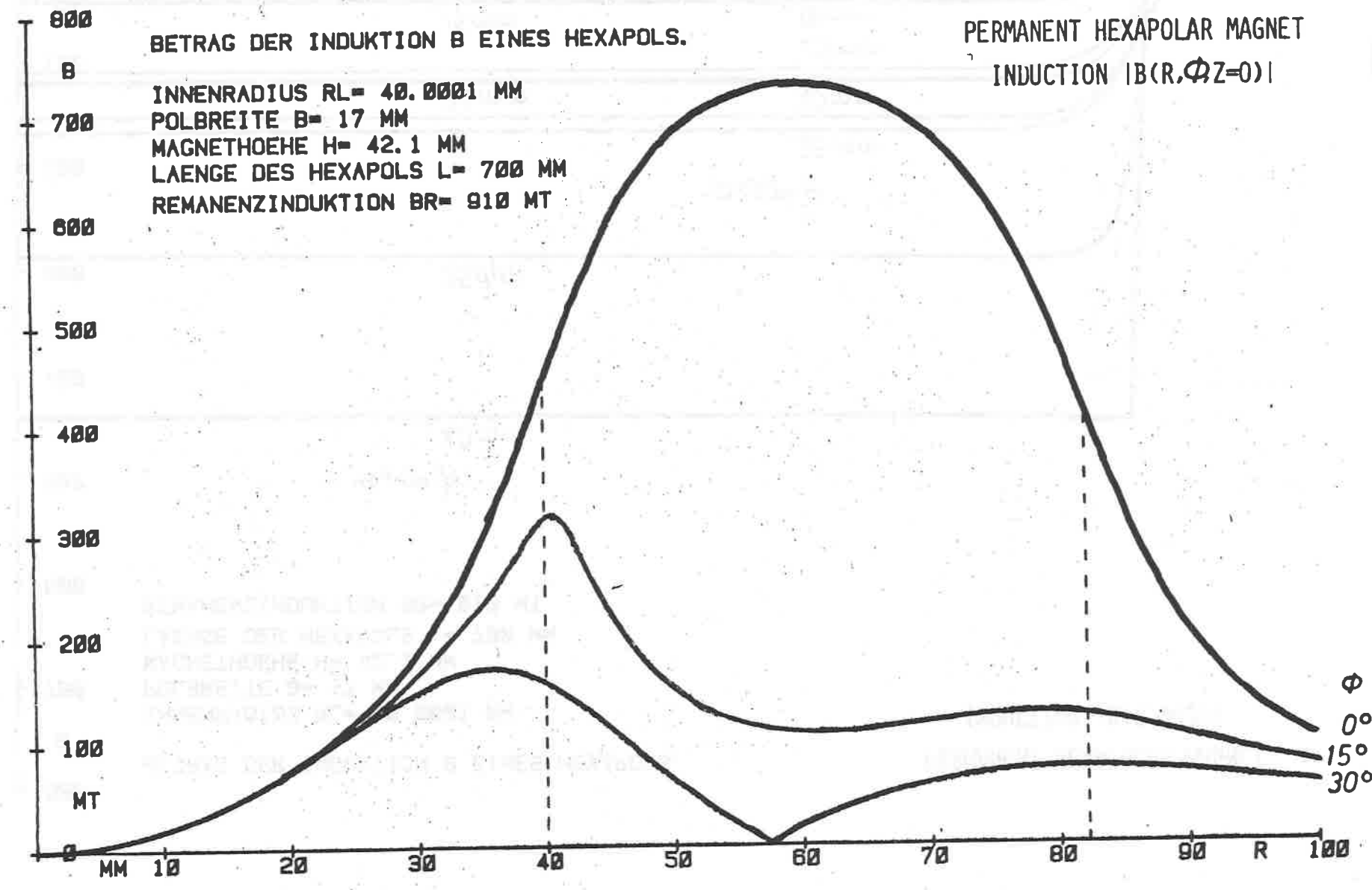
200

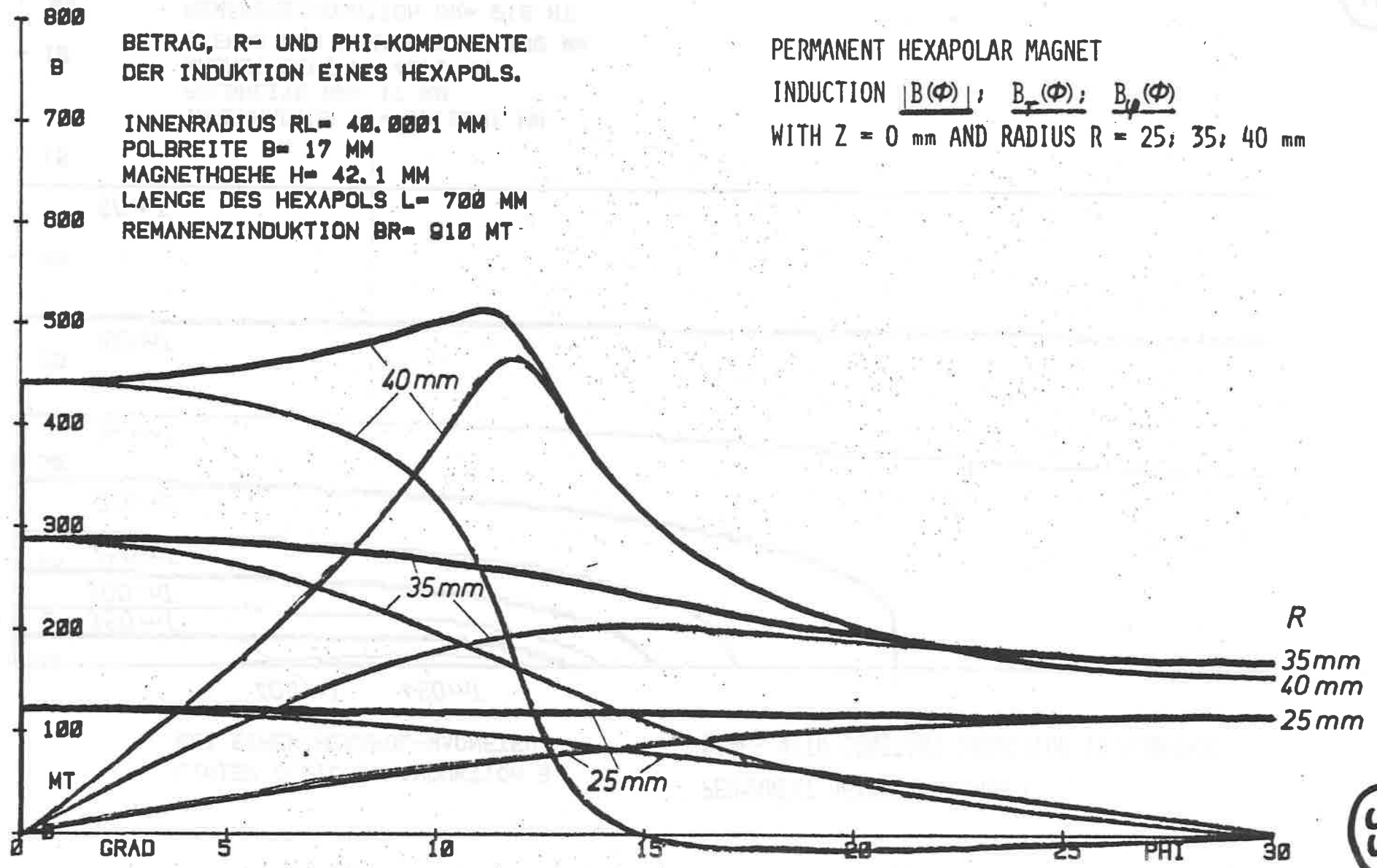
250

300

350

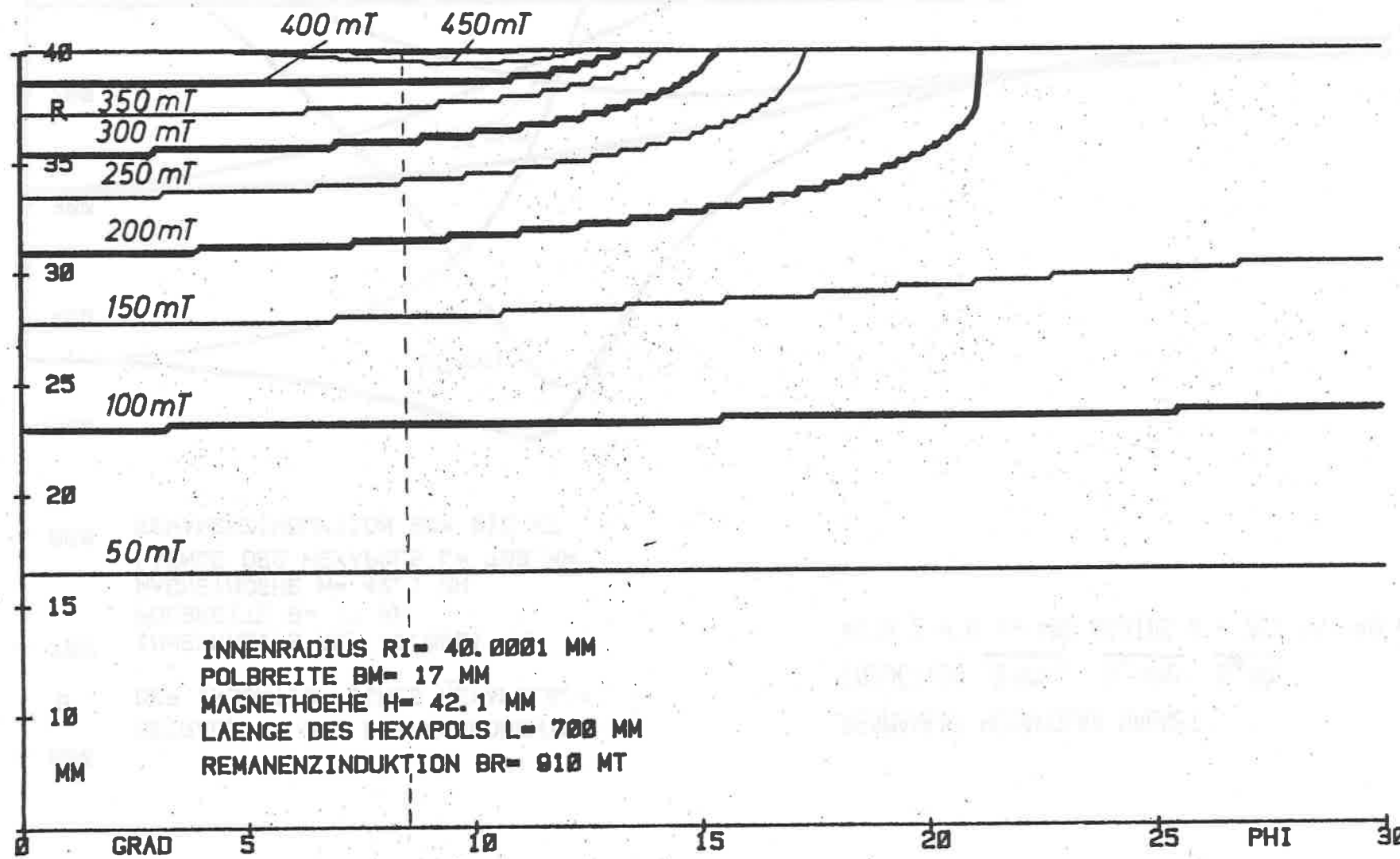
Z 400





LINIEN GLEICHER INDUKTION B
BEI EINEM HEXAPOL-MAGNETEN.

PERMANENT HEXAPOLAR MAGNET.
LINES WITH CONSTANT INDUCTION $|B(r;\phi;Z=0)|$

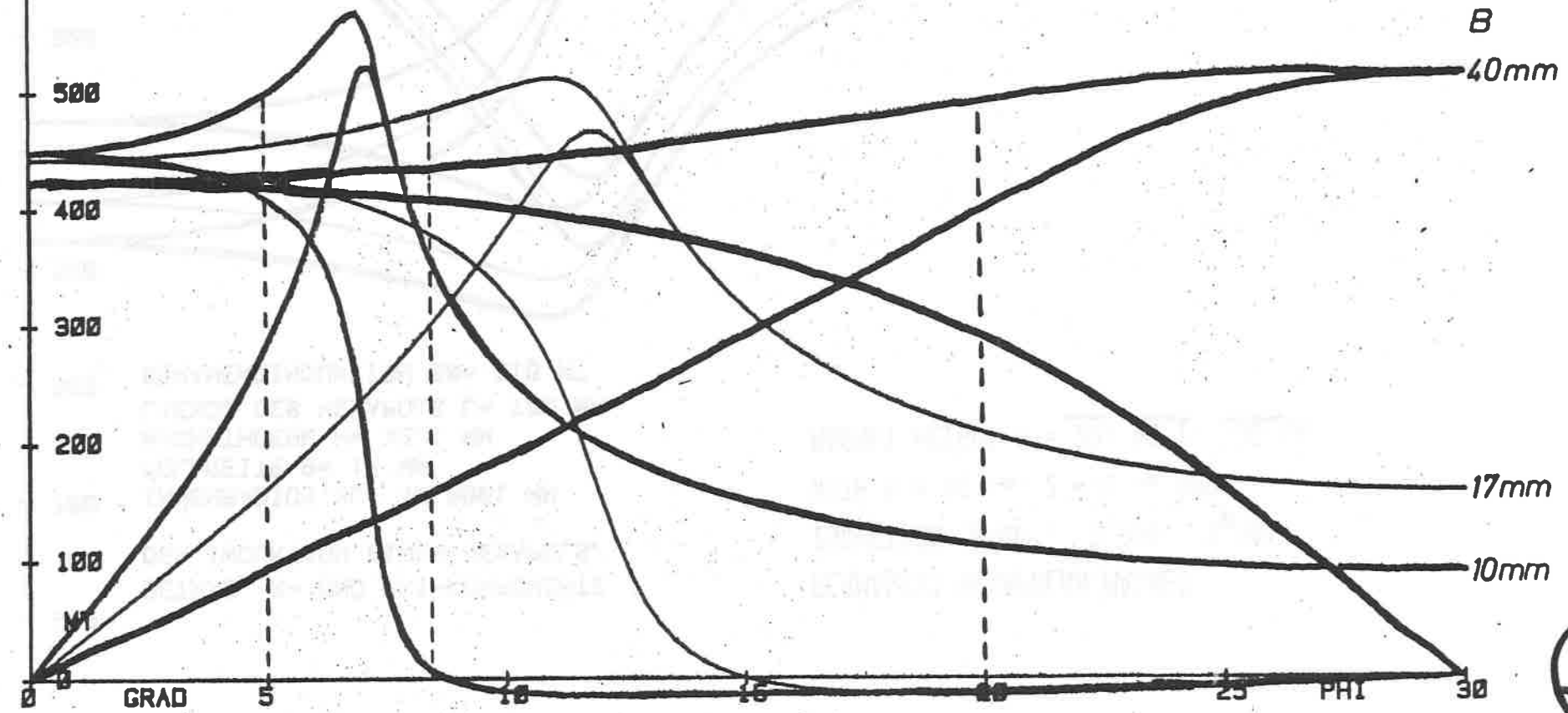


(56)

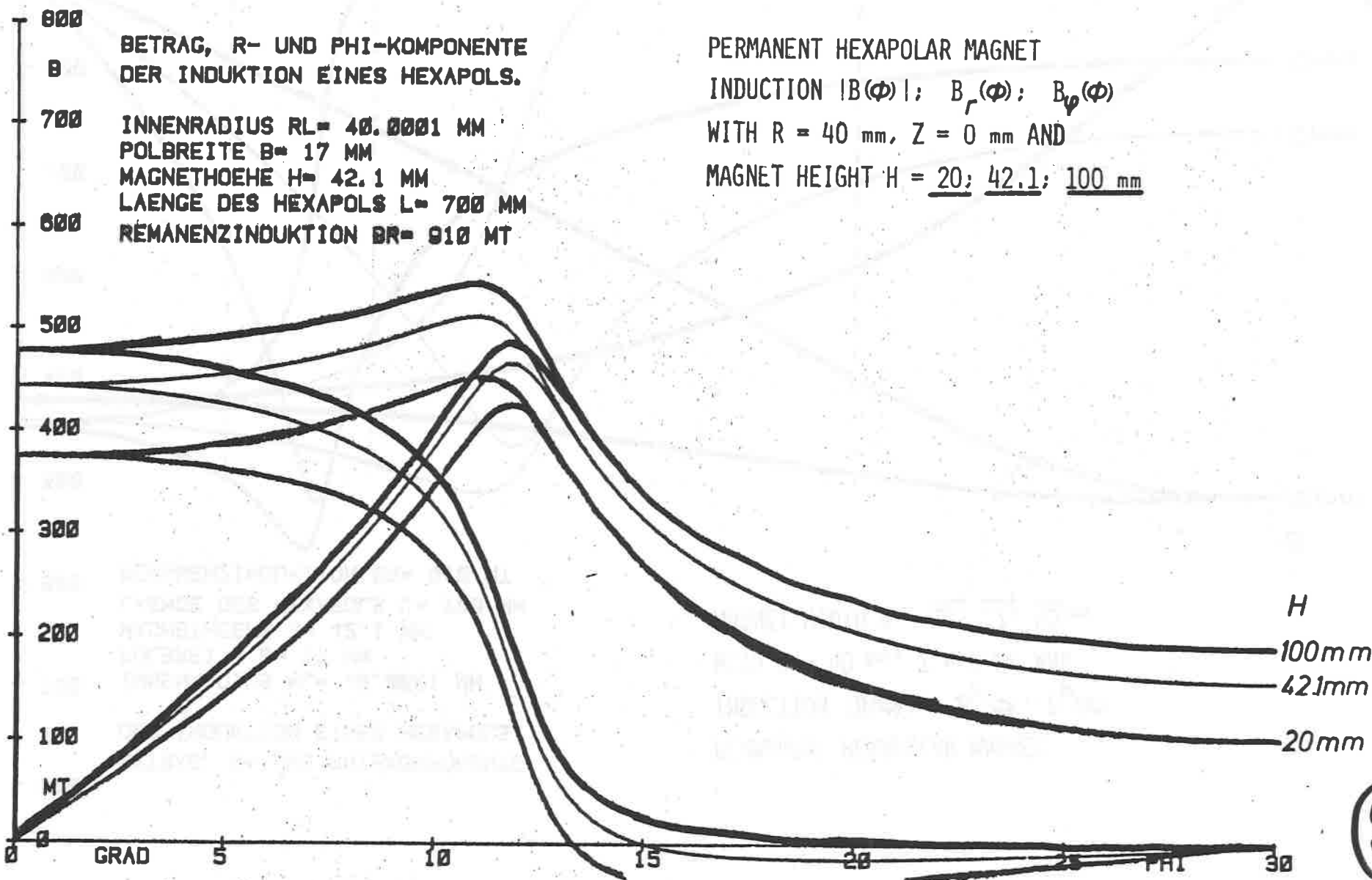
BETRAG, R- UND PHI-KOMPONENTE
DER INDUKTION EINES HEXAPOLS.

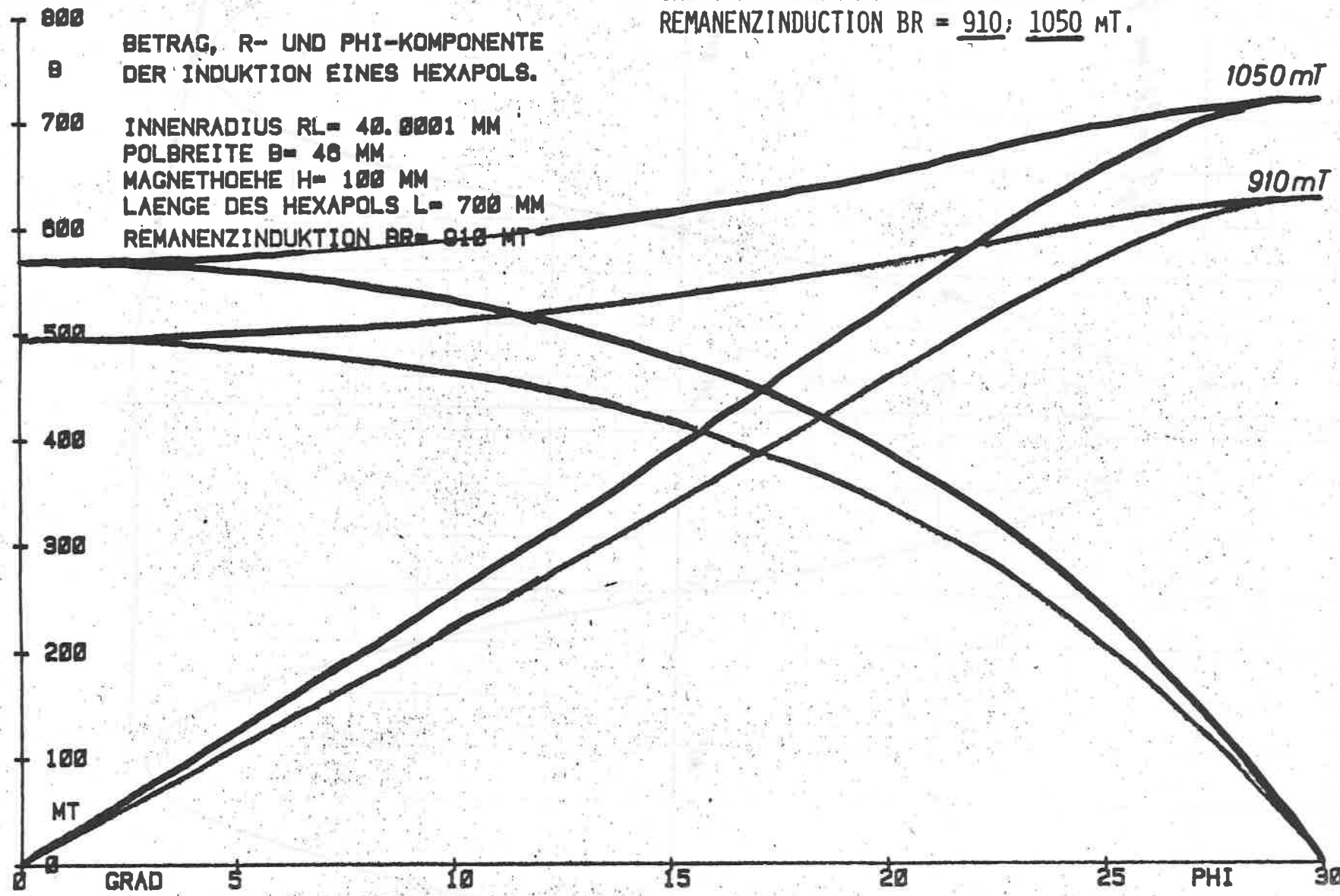
INNENRADIUS $R_L = 40.0001$ MM
POLBREITE $B = 17$ MM
MAGNETHOEHE $H = 42.1$ MM
LAENGE DES HEXAPOLS $L = 700$ MM
REMANENZINDUKTION $B_R = 910$ MT

PERMANENT HEXAPOLAR MAGNET
INDUCTION $|B(\phi)|; B_r(\phi); B_\psi(\phi)$
WITH $R = 40$ mm, $Z = 0$ mm AND
MAGNET WIDTH $B = \underline{10}; \underline{17}; \underline{40}$ mm



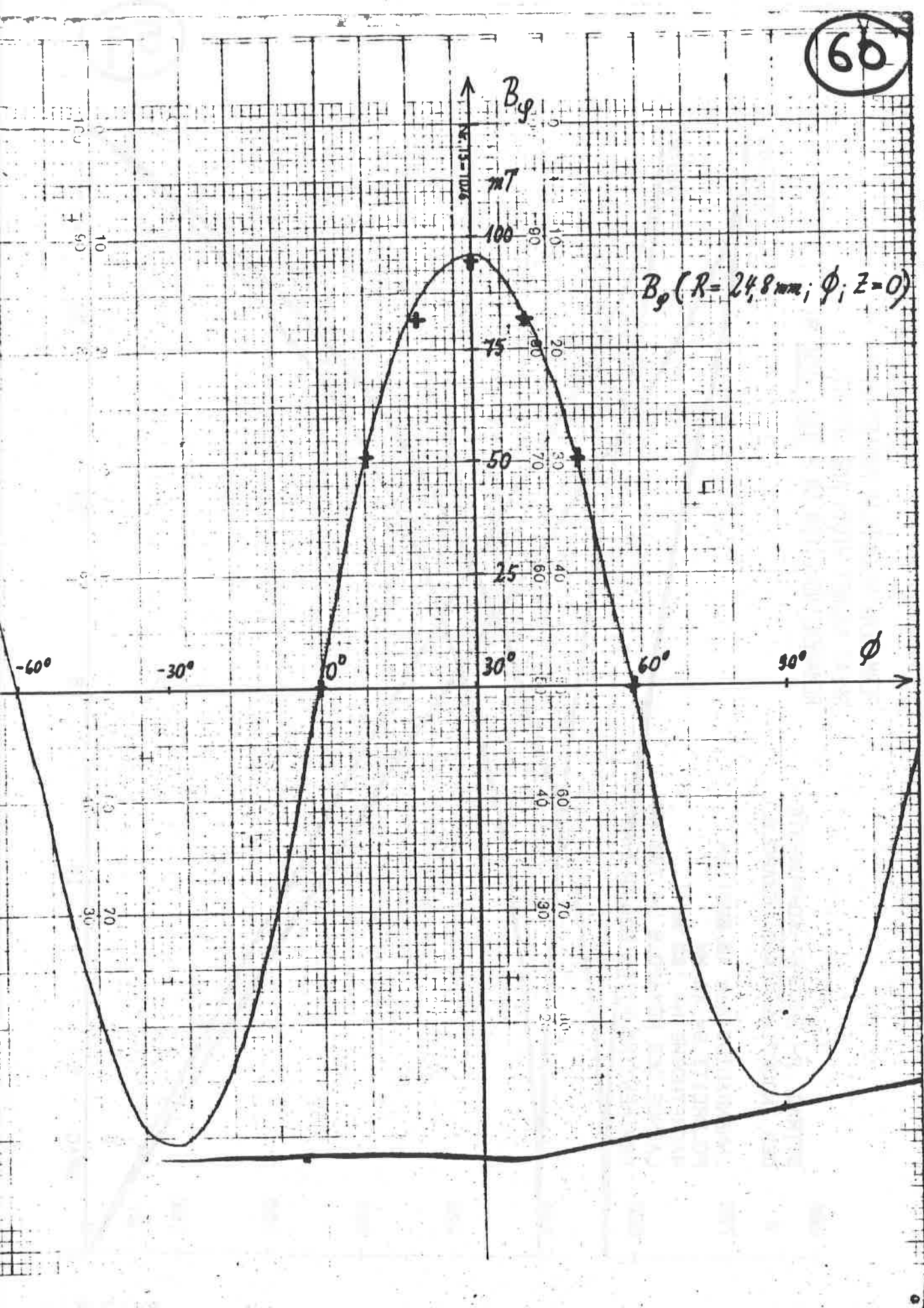
(15)



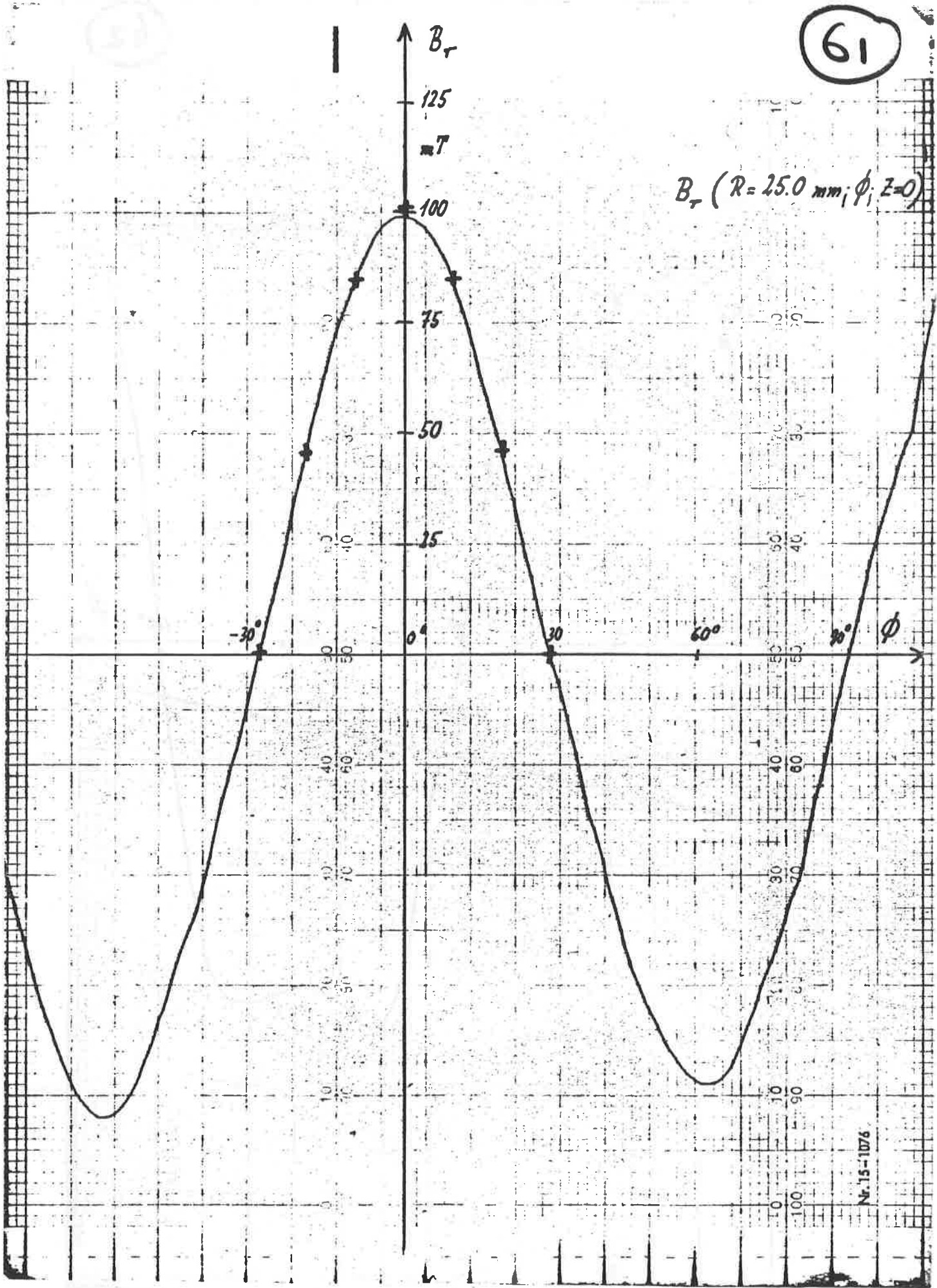


59

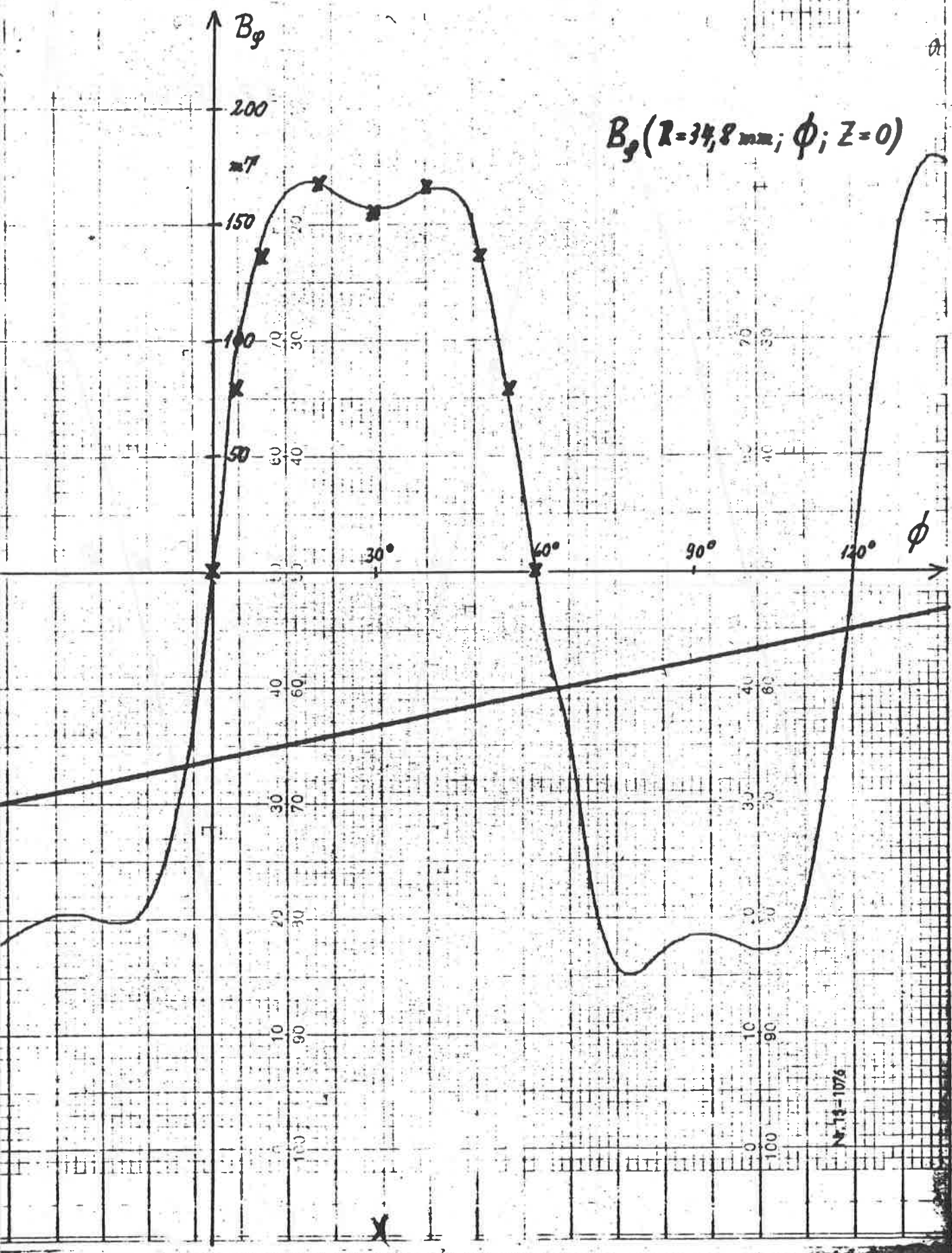
66



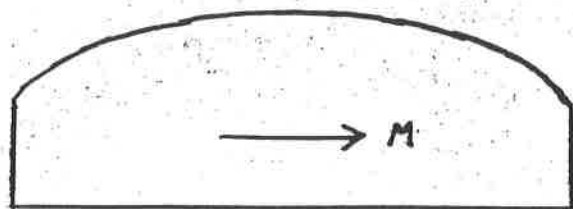
61



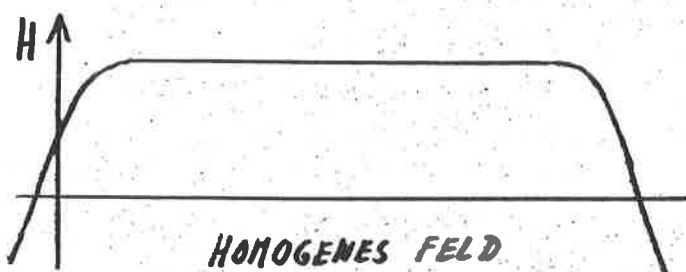
62



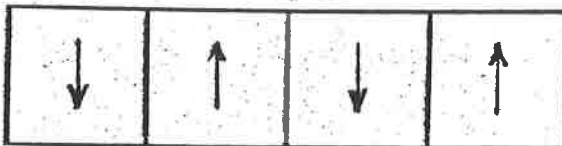
MAGNETSYSTEME FÜR WANDERFELD RÖHREN



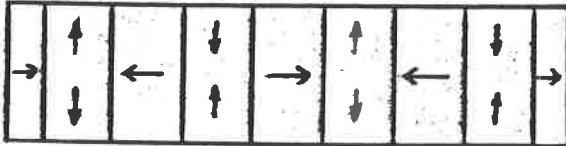
TONNENMAGNET



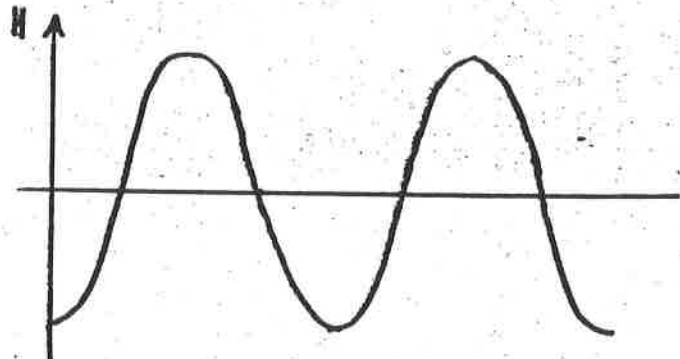
HOMOGENES FELD



RADIAL MAGNETISIERTE

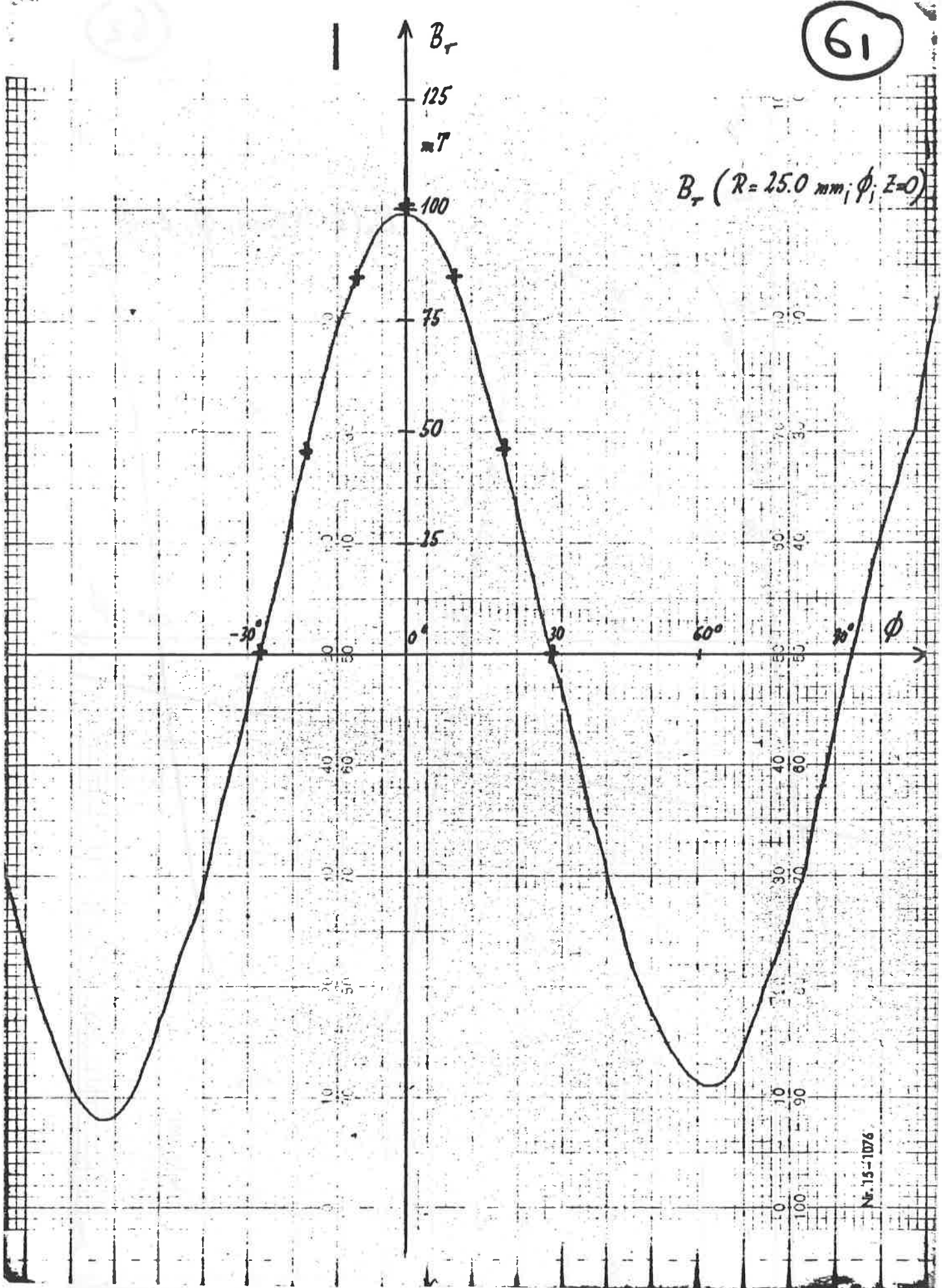


AXIAL MAGNETISIERTE

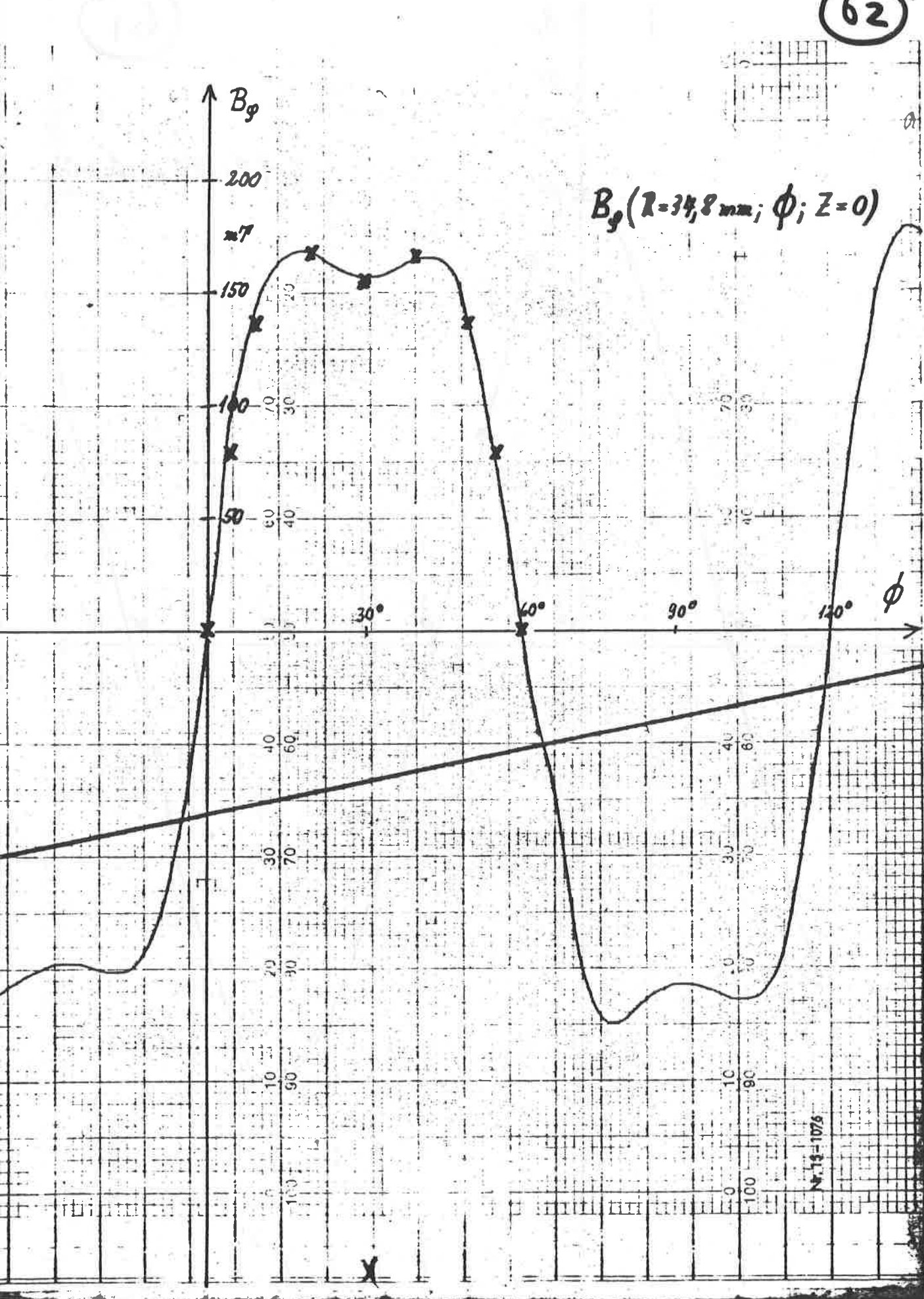


ALTERNIERENDES FELD

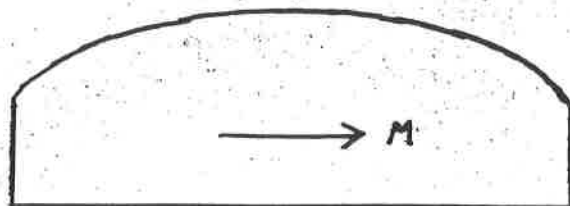
61



62



MAGNETSYSTEME FÜR WANDERFELD RÖHREN



TONNENMAGNET

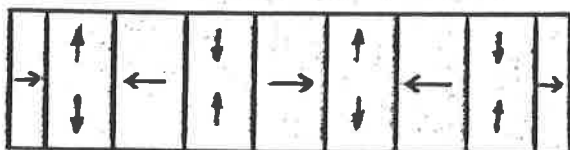


HOMOGENES FELD

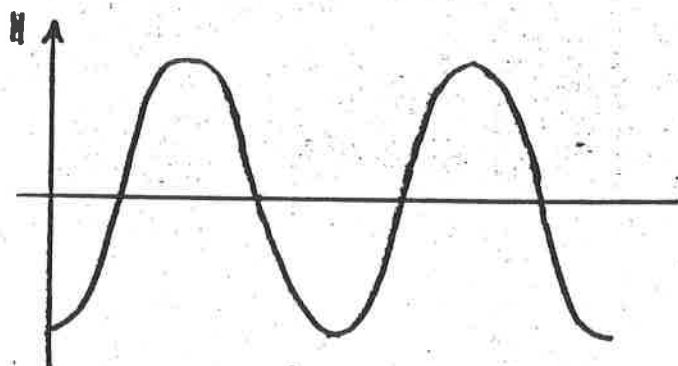


RADIAL MAGNETISIERTE

RINGE



AXIAL MAGNETISIERTE



ALTERNIERENDES FELD

